AD-A112 890 MASSACHUSETTS INST OF TECH LEXINGTON LINCOLN LAB F/G 20/5
ELECTROOPTICAL DEVICES.(U)
MAR 81 C E HURWITZ F19628-80-C-0002
UNCLASSIFIED ESD-TR-81-283 ML

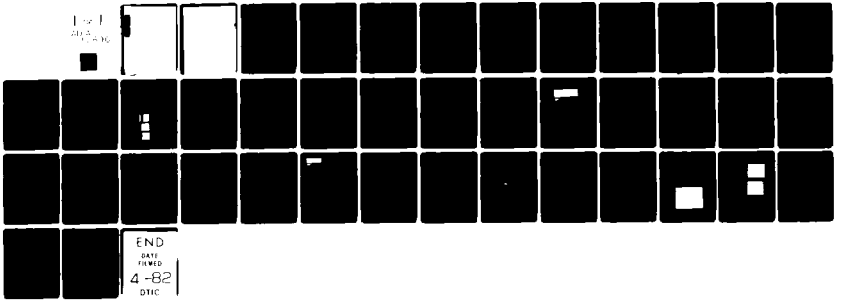

END
DATE FILMED
4-82
DTIC

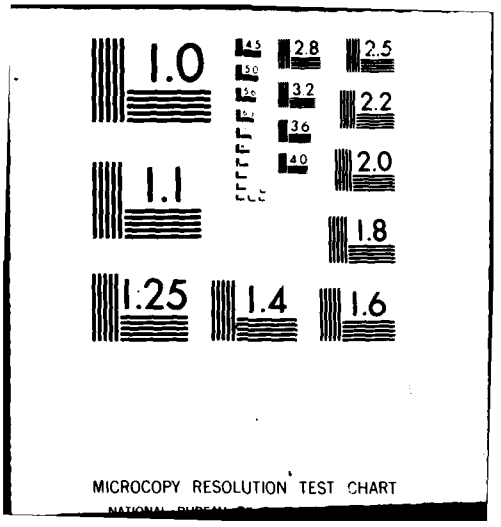
1.0
1.1
1.25
1.4
1.6
1.8
2.0
2.2
2.5
2.8
3.2
3.6
4.0
4.5
5.0
5.6
MICROCOPY RESOLUTION TEST CHART

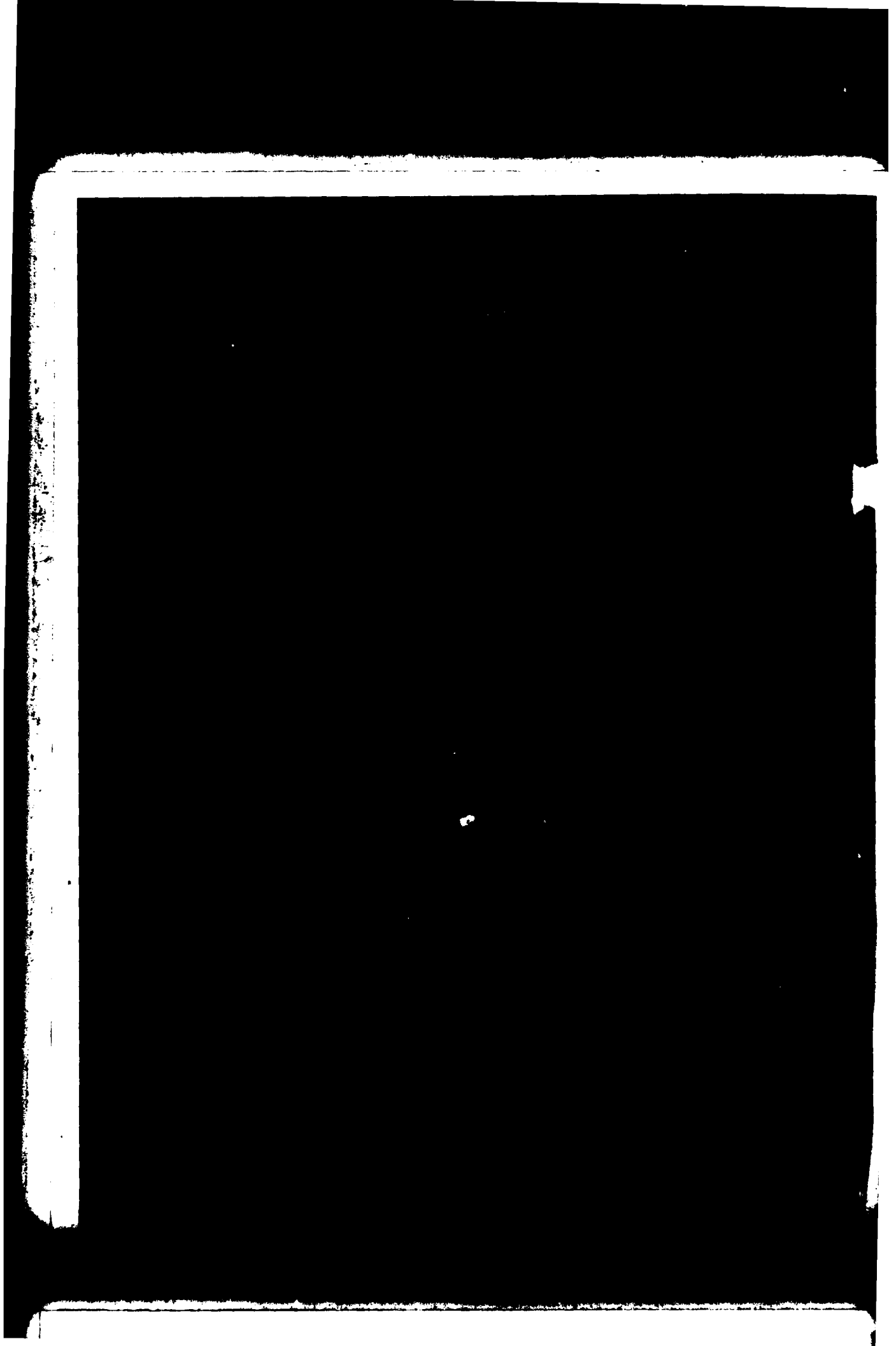

MASSACHUSETTS INSTITUTE OF TECHNOLOGY
LINCOLN LABORATORY

ELECTROOPTICAL DEVICES

SEMIANNUAL TECHNICAL SUMMARY REPORT TO THE ROME AIR DEVELOPMENT CENTER

1 OCTOBER 1980 — 31 MARCH 1981

ISSUED 25 JANUARY 1982

LEXINGTON MASSACHUSETTS

ABSTRACT

This report covers work carried out with the support of the Rome Air Development Center during the period 1 October 1980 through 31 March 1981.

The spectral dependence of the optical absorption introduced in InP and GaInAsP by proton bombardment has been measured as a function of dose. The induced absorption, which increases nearly linearly with dose, extends well beyond the band edge and decreases approximately exponentially with wavelength over a broad range. A short 420°C anneal reduces this bombardment-induced absorption by more than a factor of 10.

A study has been made of the etching technique used to delineate the active GaInAsP layer in GaInAsP/InP double-heterostructure lasers. It was found that careful control of etch solution compositions and etch time was necessary to obtain accurate measurement of active layer thickness.

A new method has been demonstrated for the prevention of thermal etching or decomposition of InP substrates prior to liquid-phase-epitaxial (LPE) growth. With this method the substrate is stored in the growth tube at room temperature during the pregrowth bake and then is transferred to the LPE slider shortly before growth. This method allows both high purity ($n \approx 1 \times 10^{15}$ cm^{-3}) and excellent surface morphology to be simultaneously and reproducibly obtained for both InP and GaInAsP LPE-grown layers.

High-quality n^+-InP layers over InGaAs have been grown from Sn solutions. The technique is generally applicable to the growth of an alloy of very low As content over one of high As content. The ability to grow these layers may facilitate the fabrication of improved InGaAs lasers and detectors operating at 1.55 μm.

CONTENTS

ELECTROOPTICAL DEVICES

I. OPTICAL PROPERTIES OF PROTON-BOMBARDED InP AND GaInAsP

Proton bombardment has been used to modify the electrical and optical properties of GaAs in many types of electrooptical and microwave devices.[1] In general, bombardment is used to create high-resistivity layers in both n- and p-type GaAs; however, the bombardment also induces an increase in optical absorption near the GaAs band edge,[2,3] an effect which may be detrimental for some electrooptical devices, particularly lasers. For many applications, a post-bombardment anneal can be used to achieve a compromise between resistivity and optical attenuation.[2,3]

The effects of proton bombardment in InP (Ref. 4) differ somewhat from those in GaAs. Very high resistivity is obtained only in p-type material and only for a narrow range of proton doses, the magnitude of which scales with the initial concentration in the InP. For sufficiently large doses, both n- and p-type InP become only moderately high resistivity n-type material. Nevertheless, proton bombardment in InP can be used effectively for some applications, including the production of current-confining regions in stripe-geometry GaInAsP/InP diode lasers.[5]

In order to optimize the design of these lasers, as well as to effectively utilize bombardment in other InP-based electrooptical devices, it is desirable to know more about the optical properties of proton-bombarded layers. We report here a study of the spectral and dose dependence of the proton-induced optical attenuation in both InP and GaInAsP ($\lambda_g \sim 1.1$ μm), and describe the effect of an anneal at moderate temperature which strongly reduces the induced attenuation. The results of these measurements are qualitatively consistent with those for GaAs.

The wafer used for these measurements consisted of a p-type InP substrate with an n-type InP buffer layer and an n-type GaInAsP layer, both grown by liquid phase epitaxy (LPE). The substrate was Cd-doped and had a hole concentration of about 10^{17} cm^{-3}. The 5-μm-thick buffer layer, which

was not intentionally doped, had an electron concentration of about 10^{17} cm^{-3}, as did the quaternary layer, which had a composition of $Ga_{0.17}In_{0.83}As_{0.4}P_{0.6}$ ($\lambda_g \sim 1.1$ μm) and a thickness of 3.5 μm. The back surface of the wafer was polished and the wafer was then cut in half. The GaInAsP epitaxial layer was chemically removed from one of the halves both to permit measurement of the InP absorption and to serve as a reference transmission to deduce the GaInAsP absorption.

For the proton bombardment and the optical transmission measurements, the two samples were mounted over holes on a common mounting plate. The samples were bombarded with a multiple-energy dose of protons to obtain nearly uniform damage throughout a 3-μm-thick bombarded layer.[4] A room-temperature bombardment schedule of N protons/cm^2 at 300 keV, 0.5 N at 200 keV, and 0.33 N at 100 keV was used for several values of N in the range 3×10^{13} $cm^{-2} \leqslant N \leqslant 3 \times 10^{15}$ cm^{-2}. After each bombardment (i.e., change in N), the transmission of the samples was measured in a commercial dual-beam spectrophotometer over the wavelength range 0.8 to 2.4 μm. The absolute transmission was determined in each case by a preliminary 100-percent transmission determination utilizing two additional mounting plates, each with holes identical to the ones in the plate on which the samples were mounted. One of these plates was left in the reference channel for the sample measurement. The accuracy of the transmission measurements with this technique is believed to be ±1 percent.

The attenuation coefficients α_1 and α_2 of the InP and the quaternary layer, respectively, prior to bombardment were calculated from standard expressions for optical transmission. For these calculations, values for the reflectivity of the materials as a function of wavelength were calculated from the values of refraction index reported in the literature,[6,7] and the small reflection at the InP/GaInAsP interface was neglected. The band-edge attenuation vs wavelength for unbombarded InP and GaInAsP is shown in Figs. I-1(a) and (b), respectively. In Fig. I-1(a), additional data from the review paper by Seraphin and Bennett[6] are shown for comparison. Our absorption edge is shifted to a longer wavelength than theirs by approximately 130 Å. The reasons for this discrepancy are not completely understood, although possible differences in

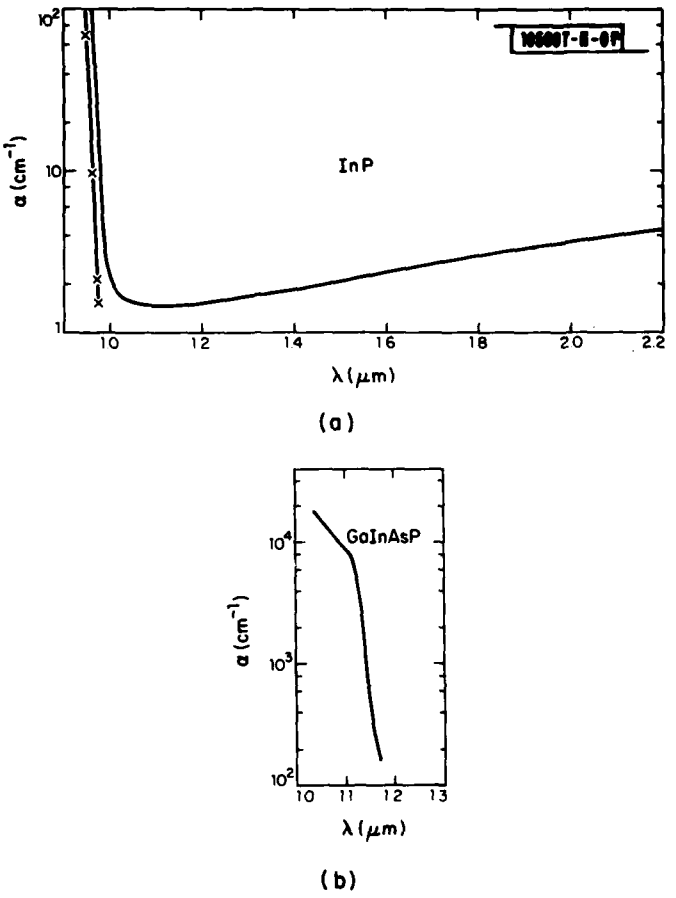

Fig. I-1. Measured absorption vs wavelength for unbombarded (a) InP and (b) $Ga_{0.17}In_{0.83}As_{0.4}P_{0.6}$. The data denoted by "X" in (a) are taken from Ref. 6.

sample temperature could account for most of the difference. In our case, the sample was heated to about 30°C above room temperature because, in the spectrometer used, all the spectral components of the source light were continuously incident on the sample. The small ($\alpha < 2$ cm^{-1}) attenuation in the 1- to 1.3-μm range is characteristic of low-concentration p-type InP (Ref. 8).

For the quaternary data, it is interesting to note the change in slope of α vs λ at $\lambda \approx 1.11$ μm. A similar effect occurs in InP near the band gap ($\lambda_g = 0.92$ μm) (Ref. 6) and in other III-V compounds,[9] and it seems reasonable

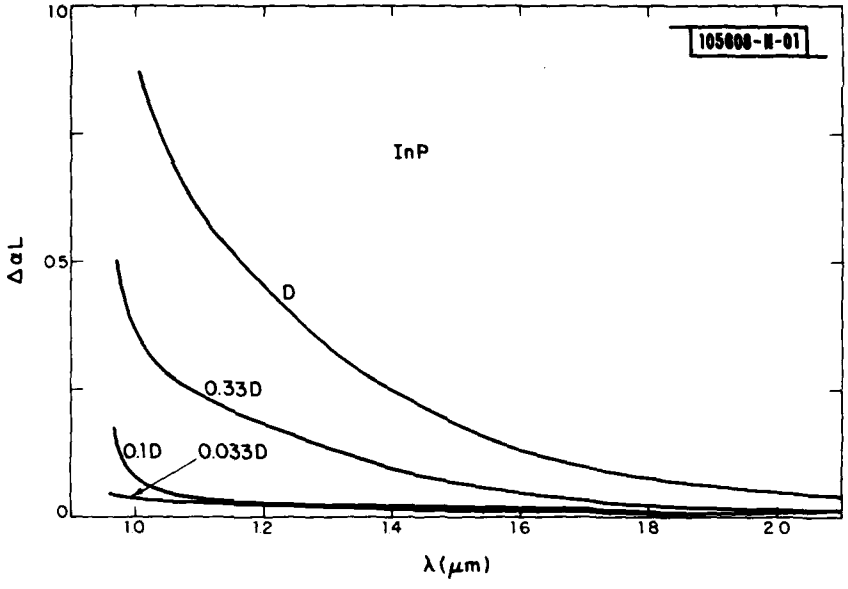

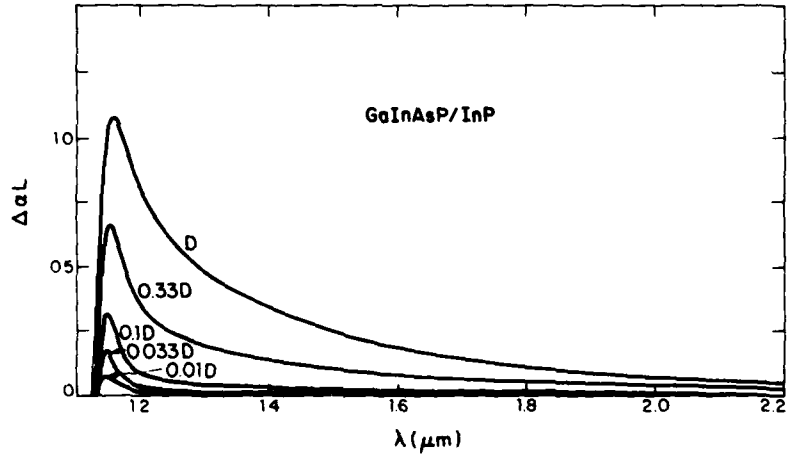

Fig. I-2. Measured bombardment-induced attenuation exponent $\Delta\alpha L$ vs wavelength with total proton dose as parameter for (a) InP and (b) $Ga_{0.17}In_{0.83}As_{0.4}P_{0.6}$. The curves are labelled with respect to a reference dose D, defined in the text for each case.

to conclude that the band gap of this quaternary is about 1.11 μm. This contrasts with a value of 1.14 μm deduced by taking the band gap to be the point where the transmission drops to 50 percent of T_{max}, which is another common method of determining the band gap.[10]

After proton bombardment, we must add to the attenuation exponents in the conventional transmission expressions a term $\int \Delta\alpha(x)dx \sim \Delta\alpha L$, where $L \sim 3$ μm, the damage depth, and $\Delta\alpha$ is the average damage-induced attenuation coefficient. [$\Delta\alpha(x)$ should be approximately constant with depth for our case of a nearly uniform damage profile.] Using the prebombardment values of α_1 and α_2 and the post-bombardment transmission, we can then solve for $\Delta\alpha L$, assuming the change in reflectivity due to the bombardment is negligible. It should be noted (see Fig. I-1) that values of α up to a factor of 100 times higher can be measured for the thin GaInAsP layer than for the InP sample.

The spectral dependence of $\Delta\alpha L$ for InP and GaInAsP is shown in Figs. I-2(a) and (b), respectively, with the normalized proton dose as parameter. The reduction of the data to obtain these curves was computer assisted. The proton doses were normalized to D, which is the total dose using the implant schedule discussed above with $N = 3 \times 10^{15}$ cm^{-2}. As shown in Fig. I-2(a), there is substantial attenuation at $\lambda = 1.3$ μm, a common lasing wavelength, for doses greater than 0.33 D. The minimum resolvable change in attenuation for InP, $\Delta\alpha L \sim 2 \times 10^{-2}$, corresponds to an ~1-percent change in transmission, the instrument accuracy, out of ~50-percent total transmission. This degree of uncertainty could account for possible errors in the tails of the 0.1 D and 0.033 D curves.

The data for GaInAsP [Fig. I-2(b)] show similar behavior to those for InP, with induced attenuation extending well beyond the band edge and with values of $\Delta\alpha \sim 3 \times 10^{3}$ cm^{-1} near the band gap. An interesting aspect is the maximum in $\Delta\alpha L$ at a wavelength of ~1.15 μm. If the curve were continued to short enough wavelengths, the values of $\Delta\alpha L$ would go negative at the band gap due to a decrease in the absorption coefficient above the band edge. These data are not plotted here due to the scatter in the results between the various bombardments. However, the effect is consistent with that seen experimentally and theoretically for other induced band-edge absorption mechanisms such as

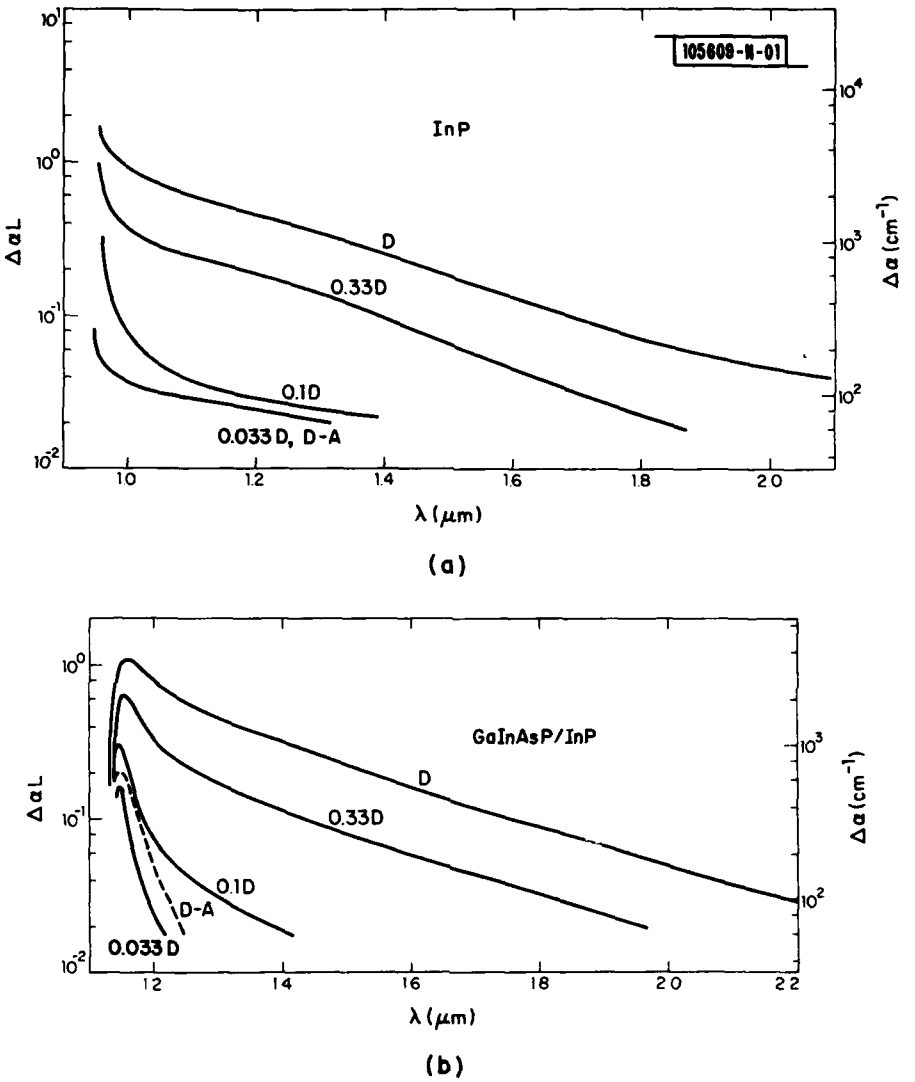

Fig. I-3. Semi-log plot of measured bombardment-induced attenuation exponent $\Delta\alpha L$ and uniform attenuation coefficient $\Delta\alpha$ vs wavelength with proton dose as parameter for (a) InP and (b) $Ga_{0.17}In_{0.83}As_{0.4}P_{0.6}$. The reference dose D is defined in the text. Also shown in each case is a curve "D-A" indicating attenuation following bombardment of dose D and a 5-min. 420°C anneal described in the text.

electroabsorption[11] (Franz-Keldysh effect). This dramatic wavelength variation in induced absorption is not measurable on the InP samples, or in previously reported GaAs studies, because the large band-edge absorption of the relatively thick substrates totally masks the changes.

The bombardment-induced absorption is replotted on a semi-log scale in Figs. I-3(a) and (b) for the InP and the GaInAsP samples, respectively. These curves show more clearly that the induced attenuation is exponentially dependent on wavelength. At doses of D and 0.33 D, one can model the attenuation as $\Delta\alpha \sim e^{-A\lambda}$ with $A = 3.1\ \mu m^{-1}$ at wavelengths $\lambda > \lambda_g + 0.2\ \mu m$ for both materials. An approximately linear dose dependence is also evident for wavelengths within ~0.1 μm of the band gap for both cases. For longer wavelengths, it is difficult to scale values of $\Delta\alpha L$ for doses from 0.1 and 0.33 D due to the limited measurement accuracy. However, between the doses of D and 0.33 D, the change in $\Delta\alpha L$ is about a factor of 3 over a broad wavelength range.

The effect of a modest anneal on reducing $\Delta\alpha$ is shown in Figs. I-3(a) and (b) by the curve labelled "D-A." This corresponds to annealing the sample bombarded with total dose D at 420°C for 5 min. in a H_2 atmosphere. As can be seen, the attenuation is reduced by more than a factor of 10, to a level for the InP sample comparable to a bombardment of 0.033 D and for the GaInAsP sample comparable to a dose of approximately 0.05 D. This anneal corresponds to the heat treatment typically used for alloying ohmic contacts in our fabrication of proton-defined stripe-geometry lasers.[5] It is therefore significant that this heat treatment greatly reduces $\Delta\alpha$ in the InP at a typical quaternary laser wavelength of 1.3 μm. These results suggest that one should be able to optimize the proton dose and anneal of GaInAsP diode lasers to maintain current confinement and minimize optical attenuation as has been done in GaAs (Ref. 2).

A comparison of the data for $\Delta\alpha$ vs dose and wavelength obtained in this work with that for GaAs (Refs. 2 and 3) indicates qualitative agreement. It is difficult to compare exactly the amount of proton-induced absorption at a given dose in the two materials because only single-energy protons were used in the GaAs work. Nevertheless, it appears that the attenuating exponent $\Delta\alpha L$ in InP and in the quaternary alloy is ~60 percent of the corresponding value in GaAs.

We have also found that GaAs tends to exhibit an exponential wavelength dependence $\Delta\alpha \sim e^{A\lambda}$, but with $A = 2.2\ \mu m^{-1}$ (Ref. 12).

F. J. Leonberger
J. N. Walpole
J. P. Donnelly
Z. L. Liau
G. W. Iseler

II. CHEMICAL ETCHING OF CLEAVED FACETS OF THE GaInAsP/InP DOUBLE HETEROSTRUCTURE

The thickness of the GaInAsP active layer, which is generally 0.1 to 0.5 μm, is an important parameter in GaInAsP/InP double-heterostructure lasers.[13-17] For an accurate measurement it is necessary to delineate the active layer in the cleaved facets by chemical etching. Perhaps the most commonly used etchant is the aqueous solution of KOH and $K_3Fe(CN)_6$, which preferentially etches the GaInAsP active layer.[13, 15, 17] However, there exists the possibility of over-etch (i.e., some etching of the InP cladding layer), which can result in an apparent active layer thickness which is greater than the actual value. We have found in this work that considerable over-etch can indeed occur for the commonly used etching conditions and have determined the conditions required to minimize over-etch.

The GaInAsP/InP wafer was prepared by sequential LPE growths of a Sn-doped InP buffer layer ($n \cong 2 \times 10^{18} cm^{-3}$), a nominally undoped GaInAsP active layer (with nearly exact lattice match to InP), a Zn-doped InP cladding layer ($p \cong 2 \times 10^{17} cm^{-3}$), and a more heavily Zn-doped InP cap layer ($p \cong 3 \times 10^{18} cm^{-3}$) on an (100) InP substrate (Sn-doped, $n \cong 1.5 \times 10^{17} cm^{-3}$). The active layer was 0.18 μm thick; the thickness of the buffer layer and that of the sum of the cap plus cladding layer were both ~4 μm. Broad-area lasers fabricated from similar wafers have shown threshold current densities as low as 0.9 kA/cm^2 with an emission wavelength of 1.3 μm. The wafer was 1.0 × 1.5 cm^2 and was cleaved into some 20 strips for various etching tests. To prepare etching solutions, weighed amounts of KOH and $K_3Fe(CN)_6$ were first separately dissolved into deionized water to form solutions of known concentrations. The two solutions were then homogeneously mixed to form etching solutions. Four different etching solution compositions were used in this work, as shown in Table II-1. (The concentrations quoted in Table II-1 are those in the final mixture.)

Figure II-1 shows scanning electron microscope (SEM) micrographs of an unetched sample and two etched ones. It should be noted that the etched

TABLE II-1

ETCHING SOLUTIONS USED IN THIS WORK AND THEIR RATES OF OVER-ETCH

Solution	$[K_3Fe(CN)_6]$	[KOH]	Increase of Apparent Active Layer Thickness
1	0.030 M	1.5 M	8.4 Å/s
2	0.0076	1.5	4.0
3	0.076	1.5	16.0
4	0.030	3.0	36.5

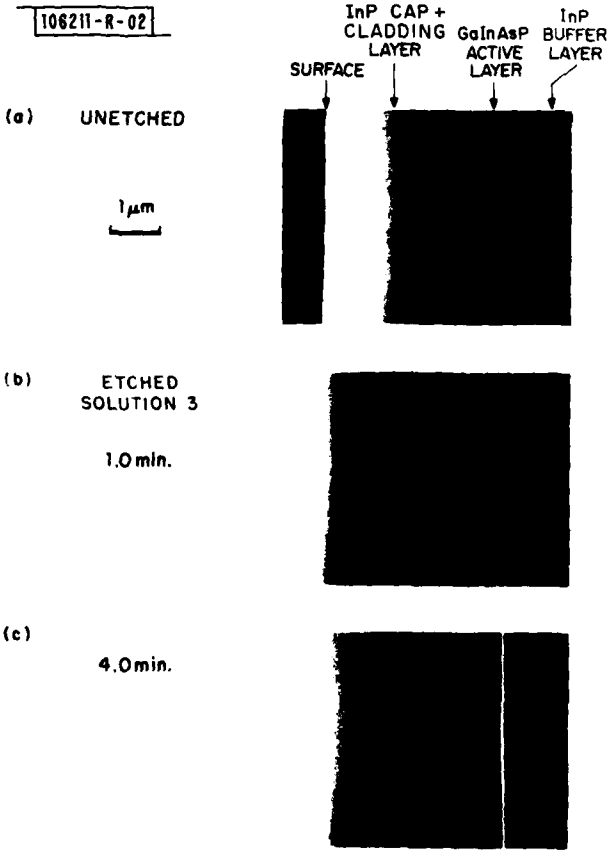

Fig. II-1. SEM micrographs of cleaved edges of an unetched sample and two etched ones. These samples were cleaved from the same LPE wafer.

samples show apparent active layer thicknesses which are considerably greater than that of the unetched one, and yet the layer boundaries still remain very sharp (i.e., no direct evidence of over-etch). The apparent active layer thickness was measured with the SEM at various positions across the length of each cleaved strip. Figure II-2 shows the results of such measurement for a series of strips etched in Solution 3. The average of apparent active layer thicknesses of each strip was then plotted against etching time, as shown in Fig. II-3. Figure II-3 shows that for each etching solution the apparent active layer thickness increases linearly with etching time. The slopes are the rates of thickness increase as quoted in Table II-1.

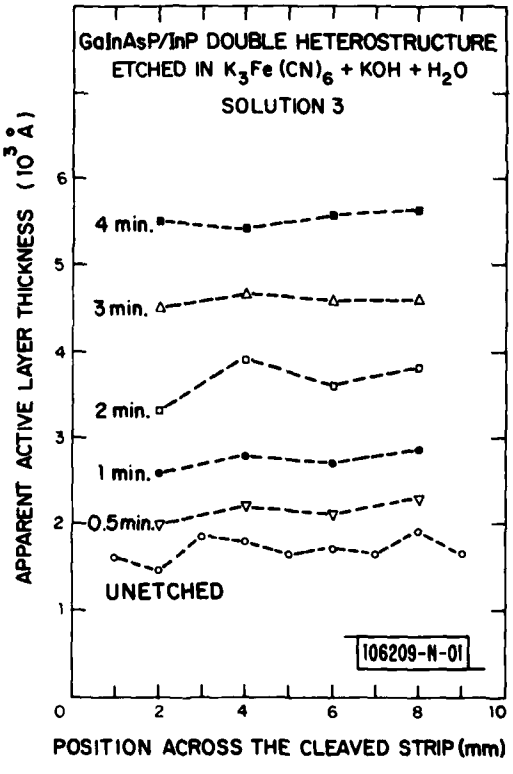

Fig. II-2. Apparent active layer thicknesses measured at various positions across a series of cleaved strips which have been etched for different lengths of time.

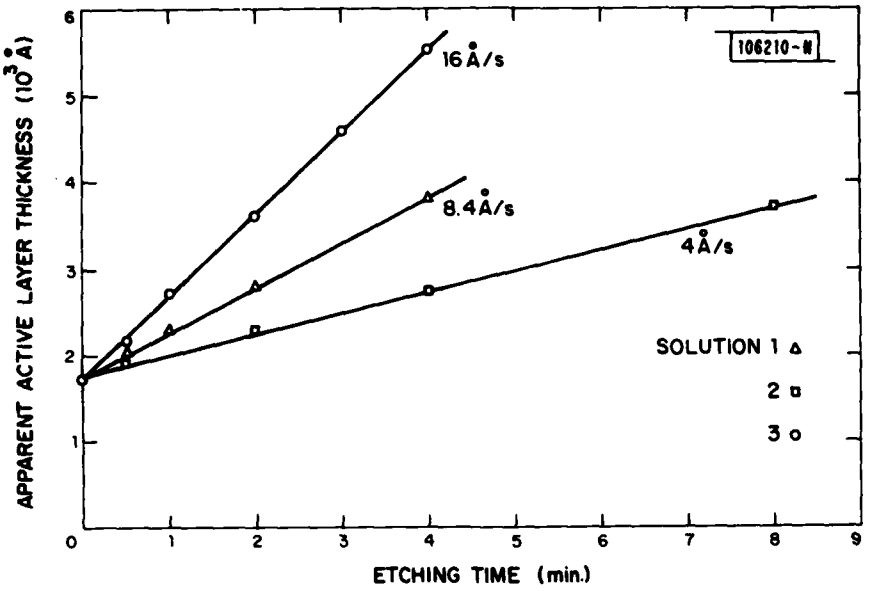

Fig. II-3. Apparent active layer thickness as a function of etching time for three different etching solution compositions.

It should be noted that rates of increase of apparent active layer thickness as high as 36.5 Å/s were obtained in the present investigation; yet the concentrations of $K_3Fe(CN)_6$ and KOH used in this work were comparable with those quoted in the literature.[18] In view of these results, we feel that some of the previously published data concerning laser characteristics, which depend on active layer thickness measurement, e.g., the normalized threshold current densities, are open to question. (We found that none of the published work which employed chemical etching for active layer measurement specified the etching conditions.) Based on the present work, low etching solution concentrations and short etching times (<10 s) should be used in order to reduce the over-etch to negligible amounts.

Z. L. Liau
T. A. Lind
L. Missagia
D. E. Mull
J. N. Walpole

III. SUBSTRATE TRANSFER TECHNIQUE FOR LPE GROWTH

A new method has been demonstrated for preventing thermal etching, or decomposition, of InP substrates prior to liquid-phase-epitaxial (LPE) growth. With this method, the substrate is stored in the growth tube, but at room temperature, during the pregrowth bake and then is transferred to the LPE slider shortly before growth. This technique requires only a modest increase in apparatus complexity and, for the most part, is straightforward in concept and use. There is one subtlety, however, which yields some information about a source of contamination in the LPE growth process, as discussed below.

Long-term baking of growth solutions is necessary to reduce the net donor concentration in LPE-grown InP and InGaAsP alloys below the 1×10^{16} cm^{-3} level. Best results are obtained when the growth directly follows this baking, i.e., without opening the system to load a substrate. For growth of InP and InGaAsP alloys of moderate phosphorus content, thermal etching of the substrate during the pregrowth bake can be prevented by introducing a gaseous source of phosphorus, usually PH_3, into the growth tube atmosphere. However, for growth of alloys of low phosphorus content, and especially for InGaAs, the phosphorus in the atmosphere quickly contaminates the growth solution.

One approach to this problem is to localize the protective phosphorus-rich atmosphere to the well of the slider containing the substrate,[19] a method that is limited to short bake times by the difficulty of providing a gas-tight well in an LPE boat. The technique we report here, of storing the substrate outside the hot zone of the furnace and then transferring it to the slider shortly before growth, is useful for indefinitely long bake times. For example, in a recent growth of InGaAs, the boat with growth and etch solutions was baked at 660°C for well over 100 hr. The substrate was transferred from its room-temperature environment within the growth tube to its normal protected position in the slider before a 30-min. pregrowth equilibration. Just prior to growth, it was slid to an open well for inspection through the transparent furnace, then slid under a pure In solution for a slight etchback,[20] and

finally slid under the growth solution. As in all our growths with this technique, there was no visual evidence of thermal degradation of the substrate at the time of the inspection, and the morphology of the epitaxial growth was excellent.

During first growths using the substrate transfer technique, the piece of graphite which served as the substrate carrier was kept at room temperature during pregrowth bake and then moved into the hot zone for the transfer. Although the growth morphology in this situation was fine, the net donor concentration was a factor of 10 to 50 larger than the 1×10^{15} cm^{-3} expected. A modified procedure incorporating two substrate carriers was then tried. One carrier, as before, held the substrate at room temperature during the pregrowth bake, but the second carrier was kept in the hot zone of the furnace. To make the transfer, the baked carrier was moved out of the furnace and the substrate was moved into it. Then this carrier was moved back into the furnace and the transfer to the slider made. With this procedure, the expected 1×10^{15} cm^{-3} net donor levels have been reproducibly obtained.

Some progress in understanding the necessity of this second substrate carrier has come from SIMS analysis of the LPE InP. The unexpectedly high donor concentration, which occurred with the single substrate carrier, was apparently due to sulfur. There are several possible sources of sulfur, but incorporation of sulfur from the air, in the form of SO_2 for example, could explain the observed contamination behavior. The gaseous sulfur compound is likely adsorbed on the graphite when the growth system is opened to air and then readily desorbed upon baking. The sulfur initially contaminates the growth solution but is, in large part, subsequently removed by baking. (SIMS analyses of LPE-grown material with $N_d - N_a \sim 1 \times 10^{15}$ cm^{-3} give approximately equal amounts of Si and S.) In the case where the single substrate carrier was used, the epitaxial growth was made 30 min. or so after the substrate carrier was heated. This time was insufficient for removal of the sulfur and there was substantial contamination. In the two-carrier experiment, many hours of pregrowth baking followed the graphite heating. The desorbed sulfur was apparently expelled during this time and the growth with $N_d - N_a \simeq 1 \times 10^{15}$ cm^{-3} was obtained.

S. H. Groves
M. C. Plonko

IV. n^+-InP LPE GROWTH ON InGaAs

The liquid-phase technique of epitaxial growth (LPE) has proved to be well adapted to heterostructure growth of InGaAsP alloys, lattice-matched to InP, for optical-fiber communication applications. One exception to this is the growth of InP over $In_{0.53}Ga_{0.47}As$, or, more generally, the growth of an alloy of very low As content over one of high As content. This problem has become more important as emphasis has shifted from desired operation at 1.3-μm wavelength to that at 1.55 μm. Both lasers and detectors for this longer wavelength have been fabricated; however, adequate growth usually has been achieved at the expense of smaller-than-desired refractive-index and energy-gap discontinuities for lasers and the omission of a contacting window layer for detectors. These factors may have compromised performance. We report here on the growth of high-quality n^+-InP layers over InGaAs by use of Sn rather than In solutions. This technique is directly applicable to the growth of avalanche-photodiode structures.[21]

When overgrowth on InGaAs by InP from In solution is attempted, there is a rapid dissolution of the InGaAs which leads to a rough interface and poor morphology of the InP layer. (Recently, this dissolution has been attributed to rapid diffusion of As in the solution.[22]) In order to achieve good epitaxial overgrowth, it is necessary to decrease the rate of the InGaAs dissolution and/or increase the rate of deposition of InP (see Ref. 23). The former can be accomplished by lowering the growth temperature, but this reduces the solubility of InP in the In and, thus, decreases the rate of deposition. (More accurately, the reduced solubility is accompanied by a reduced temperature dependence of the solubility, which determines the rate of deposition.) Increasing the supercooling helps, but not enough to give satisfactory overgrowth from In solutions.

A comparison of the InP solubility data for various solutions[24, 25] suggests that the dissolution/deposition situation should be considerably improved for Sn solutions. Figure IV-1 shows curves from Refs. 25 and 26 together with our measurements for InP-Sn solutions. The rate of deposition of InP from

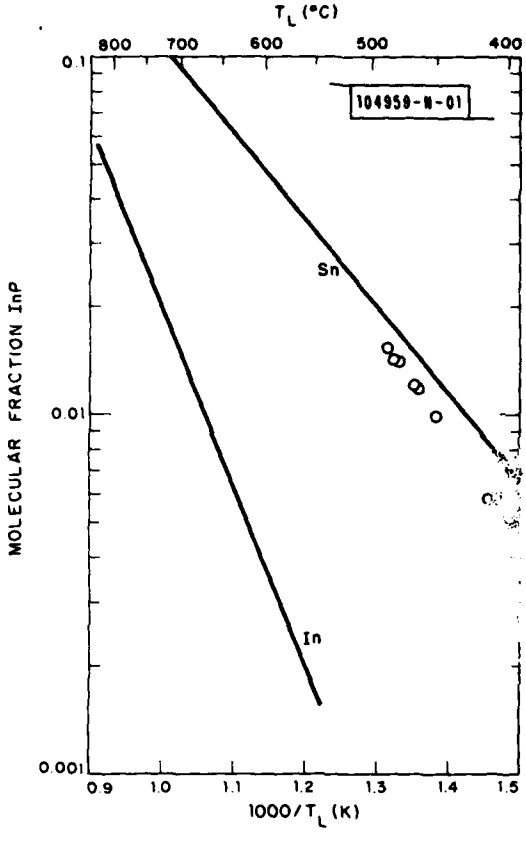

Fig. IV-1. InP solubility in Sn and In solutions. Solid line for Sn solutions is from experimental data of Ref. 25. Circles are from present experiment; because of pressure loss in our open-tube LPE system, they lie below closed-tube results of Ref. 25. For In solutions, solid line is average of data from Refs. 25 and 26.

Sn solution at 450°C, for example, is comparable to that from In solution at 700°C, and at temperatures as low as 450°C the rate of InGaAs dissolution should be much reduced.

Figure IV-2 is a photomicrograph of the cross section of a n^+-InP/InGaAs/InP structure grown using the Sn solution. The high quality of both interfaces is apparent. Because of the relatively high phosphorous pressure over the Sn solution (a property that has recently been exploited for prevention of substrate thermal decomposition[27]), this growth was made in two steps. First, the InGaAs was grown on an InP substrate at 645°C. Then, after the growth apparatus was cooled to room temperature and the components of the InP-Sn solution were added, then n^+-InP was grown at 470°C. Presumably, a capped

Fig. IV-2. Cross section of n^+-InP/InGaAs/InP growth showing high-quality interfaces for both layers of epitaxial growth.

InP-Sn solution would prevent phosphorous contamination of the InGaAs growth solution, and the double-layer growth could be made without a separate addition of the components for the n^+-InP solution. From electrical measurements made on similar n^+-InP layers grown on semi-insulating InP(Fe) substrates, the donor concentration is found to be 3.5×10^{19} cm^{-3} and the room-temperature electron mobility to be 450 $cm^2/V\text{-}s$. Within the source-broadening limitations of the single-crystal x-ray-diffraction technique, the x-ray lines of the InP(Sn) are the same as those of bulk InP.

Finally, it is noted that this technique is useful for n^+-InP/n-InGaAs/n-InP/p^+-InP inverted-mesa avalanche photodiodes, where a thin window layer of n^+-InP over the n- or n^--InGaAs is used to prevent carrier depletion to the surface. For laser structures a p-type InP overgrowth of the InGaAs (or the InGaAsP alloy with emission at 1.55 μm) is desired. Growth from Cd solution might prevent the InGaAs dissolution, but the resulting p^+-InP layer, aside from possible problems with the formation of Cd_3P_2, would have excessive free-carrier absorption loss for the laser structure. Other solutions doped

with small amounts of Zn might produce suitable layers. The reader is referred to the precautionary note by Buehler and Bachmann on the high phosphorous pressures that are present over Pb and Bi solutions.[25]

S. H. Groves
M. C. Plonko

REFERENCES

1. For review, see J. P. Donnelly, C. O. Bozler, and R. A. Murphy, Circuits Mfg. 18, 45 (1978).
2. J. C. Dyment, J. C. North, and L. A. D'Asaro, J. Appl. Phys. 44, 207 (1973).
3. E. Garmire, H. Stoll, A. Yariv, and R. G. Hunsperger, Appl. Phys. Lett. 21, 87 (1972).
4. J. P. Donnelly and C. E. Hurwitz, Solid-State Electron. 20, 727 (1977); J. P. Donnelly, to be published in Nuclear Instrument and Methods.
5. J. J. Hsieh, J. A. Rossi, and J. P. Donnelly, Appl. Phys. Lett. 28, 709 (1976).
6. B. O. Seraphin and H. E. Bennett, Vol. 3 of Semiconductors and Semimetals (Academic Press, New York, 1967), p. 527.
7. R. E. Nahory and M. A. Pollack, Electron. Lett. 14, 727 (1978).
8. G. W. Iseler (unpublished).
9. E. J. Johnson, Vol. 3 of Semiconductors and Semimetals (Academic Press, New York, 1967), p. 153.
10. M. Feng, T. H. Windhorn, M. M. Tashima, and G. E. Stillman, Appl. Phys. Lett. 32, 758 (1980).
11. R. H. Kingston, Appl. Phys. Lett. 34, 744 (1979).
12. F. J. Leonberger (unpublished).
13. J. J. Hsieh, J. A. Rossi, and J. P. Donnelly, Appl. Phys. Lett. 28, 709 (1976).
14. R. E. Nahory and M. A. Pollack, Electron. Lett. 14, 729 (1978).
15. Y. Itaya, Y. Suematsu, S. Katayama, K. Kishino, and S. Arai, Jap. J. Appl. Phys. 18, 1795 (1979).
16. S. Arai, Y. Suematsu, and Y. Itaya, IEEE J. Quantum Electron. QE-16, 197 (1980).
17. H. Kawaguchi, K. Takahei, Y. Toyoshima, H. Nagai, and G. Iwane, Electron. Lett. 15, 669 (1979).
18. M. C. Hales, J. R. Knight, and C. W. Wilkins, 1970 Symposium on GaAs (The Institute of Physics, London, 1970), p. 50.
19. G. A. Antypas, Appl. Phys. Lett. 37, 64 (1980).
20. V. Wrick, G. J. Scilla, and L. F. Eastman, Electron. Lett. 12, 394 (1976).

21. V. Diadiuk, S. H. Groves, and C. E. Hurwitz, Appl. Phys. Lett. 37, 807 (1980).

22. L. W. Cook, M. Feng, M. M. Tashima, R. J. Blattner, and G. E. Stillman, Appl. Phys. Lett. 37, 173 (1980).

23. M. Quillec and J. L. Benchimol, Proc. 1980 NATO-sponsored InP Workshop, Harwichport, Massachusetts, 17-19 June 1980, p. 207.

24. A. Leonhardt and G. Kühn, J. Less-Common Metals 37, 310 (1974).

25. E. Buehler and K. J. Bachmann, J. Cryst. Growth 35, 60 (1976).

26. J. J. Hsieh, "Thickness of InP Layers Grown by LPE from Supercooled Solutions," Chapter 2 in Gallium Arsenide and Related Compounds (St. Louis) 1976 (The Institute of Physics, London, 1977), pp. 74-80, DDC AD-A046988/2.

27. G. A. Antypas, Appl. Phys. Lett. 37, 64 (1980).

APPENDIX A

Optical Properties of Proton Bombarded InP and GaInAsP

F. J. LEONBERGER, J. N. WALPOLE, AND J. P. DONNELLY

Abstract—The spectral dependence of the optical absorption introduced in InP and GaInAsP by proton bombardment has been measured as a function of dose. A multienergy bombardment schedule was used in order to produce a uniformly bombarded layer 3 μm thick. The induced absorption, which increases nearly linearly with dose, extends well beyond the band edge and decreases nearly exponentially with wavelength over a broad range. A short 420°C anneal reduces this bombardment-induced absorption by more than a factor of ten.

PROTON bombardment has been used to modify the electrical and optical properties of GaAs in many types of electrooptical and microwave devices [1]. In general, bombardment is used to create high-resistivity layers in both n- and p-type GaAs; however, the bombardment also induces an increase in optical absorption near the GaAs band edge [2], [3], an effect which may be detrimental for some electrooptical devices, particularly lasers. For many applications, a postbombardment anneal can be used to achieve a compromise between resistivity and optical attenuation [2], [3].

The effects of proton bombardment in InP [4] differ somewhat from those in GaAs. Very high resistivity is obtained only in p-type material and only for a narrow range of proton doses, the magnitude of which scales with the initial concentration in the InP. For sufficiently large doses, both n- and p-type InP become only moderately high-resistivity n-type material. Nevertheless, proton bombardment in InP can be used effectively for some applications, including the production of current confining regions in stripe-geometry GaInAsP/InP diode lasers [5].

In order to optimize the design of these lasers, as well as to effectively utilize bombardment in other InP-based electrooptical devices, it is desirable to know more about the optical properties of proton-bombarded layers. We report here a study of the spectral and dose dependence of the proton-induced optical attenuation in both InP and GaInAsP ($\lambda_g \sim 1.1$ μm), and describe the effect of an anneal at moderate temperature which strongly reduces the induced attenuation. The results of these measurements are qualitatively consistent with those for GaAs.

The wafer used for these measurements consisted of a p-type InP substrate with an n-type InP buffer layer and an n-type GaInAsP layer, both grown by liquid-phase epitaxy (LPE). The substrate was Cd-doped and had a hole concentration of about 10^{17} cm^{-3}. The 5 μm thick buffer layer, which was not intentionally doped, had an electron concentration of about 10^{17} cm^{-3}, as did the quaternary layer, which had a composition of $Ga_{0.17}In_{0.83}As_{0.4}P_{0.6}$ ($\lambda_g \sim 1.1$ μm) and a thickness of 3.5 μm. The back surface of the wafer was polished and the wafer was then cut in half. The GaInAsP epitaxial layer was chemically removed from one of the halves to permit both measurement of the InP absorption and to serve as a reference transmission to deduce the GaInAsP absorption.

For the proton bombardment and the optical transmission measurements, the two samples were mounted over holes on a common mounting plate. The samples were bombarded with a multiple-energy dose of protons to obtain nearly uniform damage throughout a 3 μm thick bombarded layer [4]. A room-temperature bombardment schedule of N protons/cm^2 at 300 keV, 0.5 N at 200 keV, and 0.33 N at 100 keV was used for several values of N in the range of $3 \times 10^{13} \leq N \leq 3 \times 10^{15}$. After each bombardment (i.e., change in N) the transmission of the samples was measured in a commercial dual-beam spectrophotometer over the wavelength range of 0.8–2.4 μm. The absolute transmission was determined in each case by a preliminary 100 percent transmission determination utilizing two additional mounting plates, each with holes identical to the ones in the plate on which the samples were mounted. One of these plates was left in the reference channel for the sample measurement. The accuracy of the transmission measurements made using this technique is believed to be ±1 percent.

The attenuation coefficient α_1 of the InP sample prior to bombardment was computed from the transmission T_1 using the well-known relation

$$T_1 = \frac{(1 - R_1)^2 e^{-\alpha_1 x_1}}{1 - R_1^2 e^{-2\alpha_1 x_1}} \tag{1}$$

where R_1 and x_1 are the InP reflectivity and wafer thickness, respectively. Similarly, neglecting the small reflection at the InP/GaInAsP interface, the transmission T_2 of the sample with the epitaxial quaternary layer is given by

$$T_2 = \frac{(1 - R_1)(1 - R_2) e^{-(\alpha_1 x_1 + \alpha_2 x_2)}}{1 - R_1 R_2 e^{-2(\alpha_1 x_1 + \alpha_2 x_2)}} \tag{2}$$

where R_2, α_2, and x_2 are the reflectivity, attenuation, and thickness of the quaternary layer, respectively. Values for R_1 and R_2 were calculated as a function of wavelength from the values of refractive index reported in the literature [6], [7]. Equation (1) was used with the experimental transmission T_1 to obtain for unbombarded InP the attenuation versus wavelength near the band edge shown in Fig. 1(a). The values thus obtained for $\alpha_1 x_1$ were then used in (2) with the measured values of T_2 to obtain α_2 versus wavelength, which is shown in Fig. 1(b). It should be noted that values of α up to a factor of 100 times higher can be measured for the GaInAsP than for the InP sample as a consequence of the much greater thickness of the InP (280 μm versus 3.5 μm) and the minimal resolvable transmission change of 1 percent. In Fig. 1(a), data from the review paper by Seraphin and Bennett [6] are

Manuscript received February 17, 1981. This work was supported by the Department of the Air Force.

The authors are with the Lincoln Laboratory, Massachusetts Institute of Technology, Lexington, MA 021713.

0018-9197/81/0600-0830$00.75

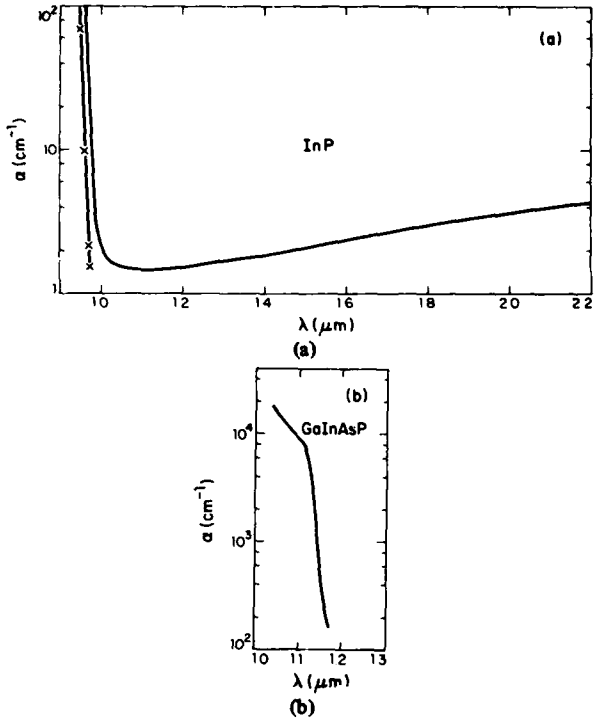

Fig. 1.

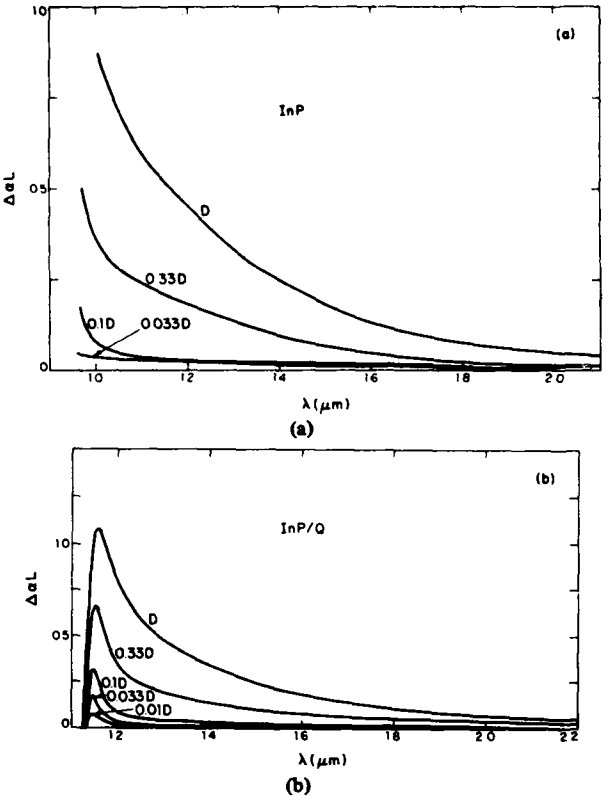

Fig. 2.

in Fig. 1(b). It should be noted that values of α up to a factor of 100 times higher can be measured for the GaInAsP than for the InP sample as a consequence of the much greater thickness of the InP (280 μm versus 3.5 μm) and the minimal resolvable transmission change of 1 percent. In Fig. 1(a), data from the review paper by Seraphin and Bennett [6] are shown for comparison. Our absorption edge is shifted to a longer wavelength than theirs by approximately 130 Å. The reasons for this discrepancy are not completely understood, although possible differences in sample temperature could account for most of the difference. In our case the sample was heated to about 30°C above room temperature because in the spectrometer used all the spectral components of the source light were continuously incident on the sample. The small ($\alpha < 2$ cm^{-1}) attenuation in the 1-1.3 μm range is characteristic of low concentration p-type InP [8].

For the quaternary data, it is interesting to note the change in slope of α versus λ at $\lambda \approx 1.11$ μm. A similar effect occurs in InP near the bandgap ($\lambda_g = 0.92$ μm) [6] and in other III-V compounds [9], and it seems reasonable to conclude that the bandgap of this quaternary is about 1.11 μm. This contrasts to a value of 1.14 μm, deduced by taking the bandgap to be the point where the transmission drops to 50 percent of T_{max}, which is another common method of determining the bandgap [10].

After proton bombardment, we must account for the proton-induced absorption by adding to $\alpha_1 x_1$ in (1), and to $\alpha_1 x_1 + \alpha_2 x_2$ in (2), a term $\int \Delta\alpha(x)dx \sim \Delta\alpha L$ where $L \sim 3$ μm, the thickness of the damaged layer, and $\Delta\alpha$ is the average damage-induced attenuation coefficient ($\Delta\alpha$ should be approximately constant with depth for our case of a nearly uniform damage profile). Using the prebombardment transmission to obtain values for $\alpha_1 x_1$ and $\alpha_1 x_1 + \alpha_2 x_2$, and using the post-bombardment transmission in (1) and (2), we can then solve for $\Delta\alpha L$, assuming the change in R_1 and R_2 due to the bombardment is negligible.

The spectral dependence of $\Delta\alpha L$ for InP and GaInAsP is shown in Fig. 2(a) and (b), respectively, with the normalized proton dose as a parameter. The reduction of the data, using (1) and (2), as described above, to obtain these curves was computer assisted. The proton doses were normalized to D, which is the total dose using the implant schedule discussed above with $N = 3 \times 10^{15}$ cm^{-2}. As shown in Fig. 2(a), there is substantial attenuation at $\lambda = 1.3$ μm, a common lasing wavelength, for doses greater than 0.33 D. The minimum resolvable change in attenuation for InP, $\Delta\alpha L \sim 2 \times 10^{-2}$, corresponds to an ~1 percent change in transmission out of ~50 percent total transmission. This degree of uncertainty could account for possible errors in the tails of the 0.1 D and 0.033 D curves.

The data for GaInAsP show similar behavior to that for InP, with induced attenuation extending well beyond the band edge and with values of $\Delta\alpha \sim 3 \times 10^3$ cm^{-1} near the bandgap. An interesting aspect is the maximum in $\Delta\alpha L$ at a wavelength of ~1.15 μm. If the curve were continued to short enough wavelengths it would actually go through zero at the bandgap due to a decrease in the absorption coefficient above the band edge. These data are not plotted here due to the scatter in the results between the various bombardments. However, the effect is consistent with that seen experimentally and theoretically for other induced band-edge absorption mechanisms such

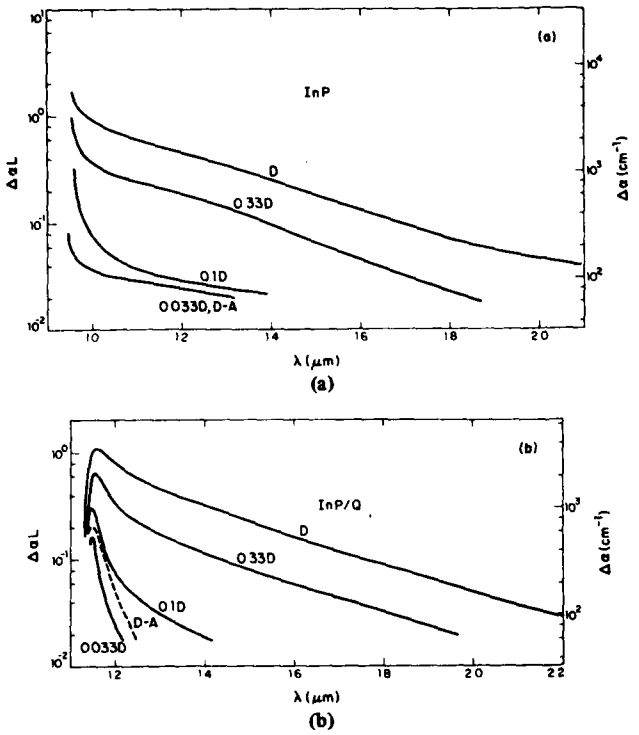

Fig. 3. Semilog plot of measured bombardment-induced attenuation exponent $\Delta\alpha L$ and uniform attenuation coefficient $\Delta\alpha$ versus wavelength with proton dose as parameter for (a) InP and (b) $Ga_{0.17}In_{0.83}As_{0.4}P_{0.6}$. The reference dose D is defined in the text. Also shown in each case is a curve *"D-A"* indicating attenuation following a bombardment of dose D and a 5-min 420°C anneal described in the text.

energy gap is not measurable on the InP samples, or in previously reported GaAs studies, because the large band-edge absorption of the relatively thick substrates totally masks the effect.

The bombardment-induced absorption is replotted on a semilog scale in Fig. 3(a) and (b) for the InP and the GaInAsP samples, respectively. These curves show more clearly that the induced attenuation is exponentially dependent on wavelength. At doses of D and 0.33 D, one can model the attenuation as $\Delta\alpha \sim e^{-A\lambda}$ with $A = 3.1$ at wavelengths $\lambda > \lambda_g + 0.2$ μm for both materials. An approximately linear dose dependence is also evident for wavelengths within ~0.1 μm of the bandgap for both cases. For longer wavelengths it is difficult to scale values of $\Delta\alpha L$ for doses from 0.1 and 0.033 D due to the limited measurement accuracy. However, between the doses of D and 0.33 D, the change in $\Delta\alpha L$ is about a factor of three over a broad wavelength range.

The effect of a modest anneal on reducing $\Delta\alpha$ is shown in Fig. 3(a) and (b) by the curve labeled *"D-A."* This corresponds to annealing the sample bombarded with total dose D at 420°C for 5 min in an H_2 atmosphere. As can be seen, the attenuation is reduced by more than a factor of 10, to a level for the InP sample comparable to a bombardment of 0.033 D and for the GaInAsP sample comparable to a dose of approximately 0.05 D. This anneal corresponds to the heat treatment typically used for alloying ohmic contacts in our fabrication of proton-defined stripe-geometry lasers [5]. It is therefore significant that this heat treatment greatly reduces $\Delta\alpha$ in the InP at a typical quaternary laser wavelength of 1.3 μm. These results suggest that one should be able to optimize the proton dose and anneal of GaInAsP diode lasers to maintain current confinement and minimize optical attenuation as has been done in GaAs [2].

A comparison of the data for $\Delta\alpha$ versus dose and wavelength obtained in this work to that for GaAs [2], [3] indicates qualitative agreement. It is difficult to compare exactly the amount of proton-induced absorption at a given dose in the two materials because only single-energy protons were used in the GaAs work. Nevertheless, it appears that the attenuating exponent $\Delta\alpha L$ in InP and in the quaternary alloy is ~60 percent of the corresponding value in GaAs. We have also found that GaAs tends to exhibit an exponential wavelength dependence $\Delta\alpha \sim e^{-A\lambda}$, but with $A = 2.2$ [12].

In summary, the spectral and dose dependences of the optical attenuation of proton-bombarded InP and $Ga_{0.17}In_{0.83}As_{0.4}P_{0.6}$ have been measured. The induced absorption extends well beyond the band edge, increases nearly linearly with dose, and, over a broad range, varies exponentially with wavelength. A short 420°C anneal has been found to greatly reduce the attenuation. The results found are qualitatively similar to those for GaAs.

Acknowledgment

The authors wish to thank G. W. Iseler and Z.-L. Liau for providing the InP substrates and the quaternary epitaxial layers, respectively. The technical assistance of H. V. Roussell, T. A. Lind, and R. C. Brooks is also gratefully acknowledged.

References

[1] For review, see J. P. Donnelly, C. O. Bozler, and R. A. Murphy, "Proton bombardment for making GaAs devices," *Circuits Manufacturing*, vol. 18, pp. 45–49, Apr. 1978.

[2] J. C. Dyment, J. C. North, and L. A. D'Asaro, "Optical and electrical properties of proton-bombarded p-type GaAs," *J. Appl. Phys.*, vol. 44, pp. 207–213, Jan. 1973.

[3] E. Garmire, H. Stoll, A. Yariv, and R. G. Hunsperger, "Optical waveguiding in proton-implanted GaAs," *Appl. Phys. Lett.*, vol. 21, pp. 87–88, Aug. 1972.

[4] J. P. Donnelly and C. E. Hurwitz, "Proton bombardment in InP," *Solid-State Electron.*, vol. 20, pp. 727–730, Aug. 1977; J. P. Donnelly, "The electrical characteristics of ion implanted compound semiconductors," *Nuclear Instr. Methods*, to be published.

[5] J. J. Hsieh, J. A. Rossi, and J. P. Donnelly, "Room-temperature CW operation of GaInAsP/InP double-heterostructure diode lasers emitting at 1.1 μm," *Appl. Phys. Lett.*, vol. 28, pp. 709–711, June, 1976; J. N. Walpole, T. A. Lind, J. J. Hsieh, and J. P. Donnelly, "Gain spectra in GaInAsP/InP proton-bombarded stripe-geometry DH lasers," *IEEE J. Quantum Electron.*, vol. QE-17, pp. 186–193, Feb. 1981.

[6] B. O. Seraphin and H. E. Bennett, "Optical properties of III–V compounds," in *Semiconductors and Semimetals*, vol. 3. New York: Academic, 1967, pp. 527–532.

[7] R. E. Nahory and M. A. Pollack, "Threshold dependence on active-layer thickness in InGaAsP/InP D.H. lasers," *Electron. Lett.*, vol. 14, pp. 727–729, Nov. 1978.

[8] G. W. Iseler, unpublished.

[9] E. J. Johnson, "Absorption near the fundamental edge," in *Semiconductors and Semimetals*, vol. 3. New York: Academic, 1967, p. 153.

[10] M. Feng, T. H. Windhorn, M. M. Tashima, and G. E. Stillman, "Liquid-phase epitaxial growth of lattice-matched InGaAsP on (100)-InP for the 1.15–1.31-μm spectral region," *Appl. Phys. Lett.*, vol. 32, pp. 758–761, June 1978.

[11] R. H. Kingston, "Electroabsorption in GaInAsP," *Appl. Phys. Lett.*, vol. 34, pp. 744–746, June 1979.

[12] F. J. Leonberger, unpublished.

APPENDIX B

n^+-InP growth on InGaAs by liquid phase epitaxy

S. H. Groves and M. C. Plonko
Lincoln Laboratory, Massachusetts Institute of Technology, Lexington, Massachusetts 02173

(Received 2 March 1981; accepted for publication 1 April 1981)

High-quality epitaxial growth of InP over InGaAs without dissolution has been achieved by using Sn-rich, rather than the more conventional In-rich, solutions. This technique, which produces n^+-InP, is directly applicable to growth of *p-i-n* and avalanche photodiode structures designed for operation in the 1.55-μm wavelength region of minimum loss in optical fibers.

PACS numbers: 81.15.Lm, 68.55. + b, 85.60.Dw, 68.48. + f

The liquid phase technique of epitaxial growth (LPE) has proved to be well suited for the growth of InGaAsP alloys lattice-matched to InP. Heterostructures of these materials have found wide application in the fabrication of lasers and detectors for optical fiber communication at 1.0–1.6 μm. One area of difficulty, however, has been the growth of InP over $In_{0.53}Ga_{0.47}As$, or, more generally, the growth of an alloy of very low As (high P) content over one of high As (low P) content, which is required for devices operating in the long-wavelength end of the range. This problem has become more important with the increasing interest in operation in the 1.55-μm region of minimum fiber attenuation. Both lasers and detectors for this longer wavelength have been fabricated; however, adequate growth usually has been achieved at the expense of smaller-than-desired refractive index and energy-gap discontinuities for lasers and the omission of a contacting window layer for detectors. These factors may have compromised performance. We report here on the growth of high-quality n^+-InP layers over InGaAs by use of Sn rather than In solutions. This technique is directly applicable to the growth of structures for *p-i-n* and avalanche photodiodes.

When overgrowth of InP on InGaAs (abbreviated as InP/InGaAs) from In solution is attempted, typically at 600–650 °C, there is a rapid dissolution of the InGaAs, which leads to a rough interface and poor morphology of the InP layer. Recently, this dissolution has been attributed to rapid diffusion of As in the solution.[1] In order to achieve good epitaxial overgrowth it is necessary to decrease the rate of the InGaAs dissolution and/or increase the rate of deposition of InP.[2] The former can be accomplished by lowering the growth temperature, but this reduces the solubility of InP in the In and thus decreases the rate of deposition. (More accurately, the reduced solubility is accompanied by a reduced temperature dependence of the solubility, which in turn lowers the rate of deposition.) Increasing the supercooling helps[3] but not enough, in our experience, to give satisfactory overgrowth from In solutions.

A comparison of the InP solubility data for various solvents[4,5] suggests that the dissolution/deposition situation should be considerably improved for Sn solutions. Figure 1 shows solubility data for InP in Sn and In taken from Refs. 5 and 6 and from our measurements for InP-Sn solutions. It is deduced from these data that the deposition rates in InP from Sn solution at 450 °C and from In solution at 700 °C are comparable. At the low temperature of 450 °C the rate of InGaAs dissolution should be much reduced. Furthermore, successful attempts to grow InP from Sn-rich solutions on InP substrates have been previously reported by Astles *et al.*[7] and by Shay *et al.*[8]

In our work, n^+-InP/InGaAs/InP structures have been successfully grown by using a conventional In solution for deposition of the InGaAs layer and a Sn solution for the n^+-InP layer. The growth is carried out in two steps. First, the InGaAs is grown on the InP substrate at 645 °C. Then, after the growth apparatus is cooled to room temperature and the components of the InP-Sn solution added, the n^+-InP is grown at ~470 °C. This procedure was adopted to avoid phosphorus contamination of the InGaAs growth solution because of the relatively high phosphorus pressure over the InP-Sn solution (a property that has recently been exploited for prevention of thermal decomposition of substrates[9]). Alternatively, a tightly capped well containing the InP-Sn solution would allow the double layer growth to be made without separately adding the components for that solution.

Figure 2 is a photomicrograph of the cross section of a n^+-InP/InGaAs/InP structure grown as described above. The high quality of both growth interfaces is apparent. Auger depth profiling measurements have been made on a similar structure, but one grown with thin epitaxial layers to reduce the sputtering time. The resulting data are shown in Fig. 3. We have been unable to accurately determine the thicknesses of the very thin layers in this particular growth

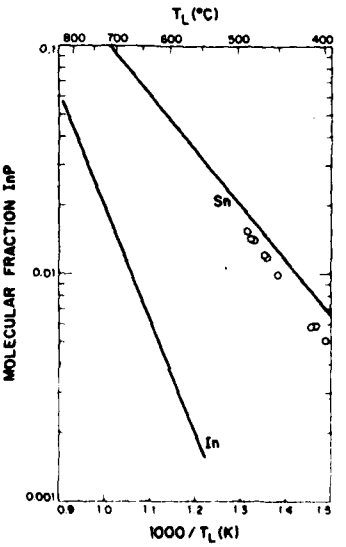

FIG. 1. InP solubility in Sn and In solutions. The solid line for Sn solutions is from the experimental data of Ref. 5. The circles are from open-tube measurements made using a "transparent," gold reflector-type furnace during this study. For In solutions, the solid line is an average of the data from Refs. 5 and 6.

 0003-6951/81/121003-02$00.50

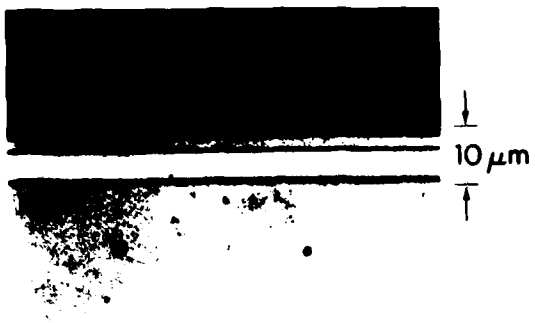

FIG. 2. Cross section of n^+-InP/InGaAs/InP growth. The InGaAs layer is about 5 μm thick and the n^+-InP is about 2 μm thick.

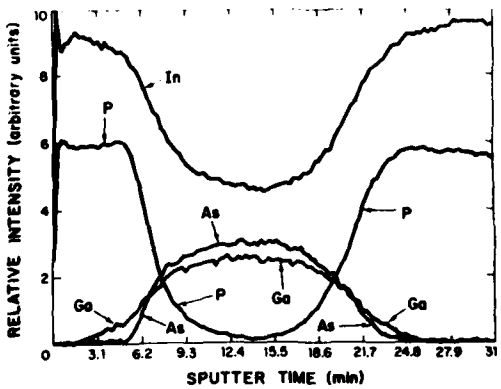

FIG. 3. Auger depth profile of an n^+-InP/InGaAs/InP stucture. Sputtering was done with 1-keV Ar^+-ion bombardment. For Auger measurements, 404, 1070, 1228, and 120-eV transitions were used for In, Ga, As, and P, respectively.

to calibrate the sputtering rate for the Auger analysis. An upper limit is ~60 Å/min from which we deduce an upper limit on the InP(Sn)/InGaAs junction width of ~200 Å. However, most of the scanning electron microscope (SEM) pictures suggest a structure thickness and thus a sputtering rate half the upper limit. This would give a junction width of ~100 Å, which is comparable to the width of the abrupt InGaAs/InP junction reported by Cook *et al.* and which may be limited by the Auger depth probe resolution under these profiling conditions.[1] The fact that the n^+-InP/InGaAs and InGaAs/InP transition widths in Fig. 3 are comparable is, in itself, evidence of the successful InP overgrowth.

Electrical measurements have been made on InP layers grown from Sn solutions on semi-insulating substrates. The donor concentration was found to be about 3.5×10^{19} cm^{-3} and the room temperature electron mobility to be about 450 cm^2/V sec, in rough agreement with values reported in Refs. 7 and 8. X-ray diffraction measurements have been made on these layers, and , within the source broadening limitations of the single-crystal x-ray diffraction technique, the x-ray lines of the InP(Sn) are the same as those of bulk InP. More accurate measurements would be necessary to reveal the lattice superdilation phenomena observed on highly doped GaAs.[10]

Finally, we note that this technique is useful for growth of structures for *p-i-n* and avalanche photodiodes, where a thin layer of n^+-InP over the InGaAs provides a transparent contact and reduces the effects of surface recombination and carrier diffusion.[11] For laser structures a *p*-type InP growth on the InGaAs (or the InGaAsP alloy with emission at 1.55 μm) is desired. Growth from a Cd solution might prevent the InGaAs dissolution, but, in addition to the possible problem of rapid Cd diffusion into the InGaAs, the resulting p^+-InP layer probably would have excessive absorption loss for the laser structure. Solutions of other elements doped with Zn might produce suitable layers. We have attempted to use Pb and Bi solutions but have found the phosphorus loss to be prohibitively large, as predicted by Buehler and Bachmann.[5]

It is a pleasure to acknowledge M. C. Finn for the Auger analysis and P. M. Nitishin for scanning electron microscope (SEM) measurements. Z. L. Liau provided assistance with SEM measurements and made helpful comments on the junction thickness determination problem. G. W. Iseler has provided substrate material and A. J. Strauss has made helpful comments on the problem of growth of InP from solutions with elements other than In as the solvent. This work was sponsored by the Department of the Air Force.

[1] L. W. Cook, M. Feng, M. M. Tashima, R. J. Blattner, and G. E. Stillman, Appl. Phys. Lett. 37, 173 (1980).
[2] M. Quillec and J. L. Benchimol, *Proceedings of the* 1980 *NATO-Sponsored* InP *Workshop*, edited by J. M. Kennedy, RADC-TM-80-07 (Hanscom AFB, Mass., 1980), p. 207. Also, to be published in J. Crystal Growth.
[3] J. J. Hsieh, Appl. Phys. Lett. 37, 25 (1980).
[4] A. Leonhardt and G. Kuhn, J. Less-Common Metals 37, 310 (1974).
[5] E. Buehler and K. J. Bachmann, J. Crys. Growth 35, 60 (1976).
[6] J. J. Hsieh, *GaAs and Related Compounds*, St. Louis, 1976 (Inst. Phys. Conf. Ser. 33b, 74, 1976).
[7] M. G. Astles, F. G. Smith, and E. W. Williams, J. Electrochem. Soc. 120 1750 (1973).
[8] J. L. Shay, K. J. Bachmann, and E. Buehler, Appl. Phys. Lett. 24, 192 (1974).
[9] G. A. Antypas, Appl. Phys. Lett. 37, 64 (1980).
[10] J. B. Mullin, B. W. Strangham, C. M. H. Driscoll, and A. F. W. Willoughby, J. Appl. Phys. 47, 2584 (1976).
[11] V. Diadiuk, S. H. Groves, and C. E. Hurwitz, Appl. Phys. Lett. 37, 807 (1980).

APPENDIX C

Journal of Crystal Growth 54 (1981) 81–87
North-Holland Publishing Company

LIQUID-PHASE EPITAXIAL GROWTH OF InP AND InGaAsP ALLOYS *

S.H. GROVES and M.C. PLONKO
Lincoln Laboratory, Massachusetts Institute of Technology, Lexington, Massachusetts 02173, USA

Liquid-phase epitaxy (LPE) has been used to grow high-quality layers of InP and InGaAsP alloys on InP substrates for a wide variety of device-development and physical-measurement applications. An apparatus featuring a transparent furnace and an atmosphere with controlled amounts of H_2, PH_3 and H_2O has proved to be flexible enough for diverse crystal growth requirements. Carrier concentration vs temperature measurements on LPE-grown InP and InGaAsP samples with $N_D - N_A$ in the low 10^{15} cm^{-3} range show that they contain a moderate concentration of deep donors. There is evidence that these deep donor states also account for a strong peak in the photoluminescence seen in LPE-grown samples. Substrate-orientation studies have shown that critically oriented substrates improve the morphology for growth of heavily Zn-doped InP.

Liquid-phase epitaxial growth of InP and InGaAsP alloys has been used in numerous applications at MIT Lincoln Laboratory. These include the development of lasers [1], avalanche photodetectors [2,3], monolithic laser-modulators [4], waveguides, microwave devices and solar cells [5]. Epitaxial structures have been grown for the measurement of ionization coefficients [6] and band structure parameters [7]. Our efforts have been devoted mainly to those applications which require low carrier concentrations.

Our growth system, shown schematically in fig. 1, is conventional in most respects but contains embellishments that have provided the flexibility needed for a laboratory-type growth system for InP and InGasP alloys. Long-term baking is of special concern, and, in this regard, it should be pointed out that both types of detector presently of interest for 1.1–1.6 μm fiber-optical applications – the InGaAsP/InP APD [3] and the InGaAs PIN detector [8] – are improved by the use of layers with carrier concentrations in or below the low 10^{15} cm^{-3} range. For LPE material long-term baking of growth solutions is needed to reduce the impurity concentration to this level.

In general, the liquidus temperature varies with time, and in our apparatus with a "transparent" furnace [9] the liquidus temperature can be determined visually. Phosphorus loss from the growth solutions can be prevented by the addition of small amounts of PH_3 to the growth tube atmosphere. Also, the PH_3 protects the substrate from decomposition [10], which permits baking with the substrate in the system for periods of 50 h or more. To achieve the lowest carrier concentrations and for the best reproducibility in baking, small amounts of O_2 are added; this readily converts to H_2O in the hot growth tube. The composition of a mixture of H_2, PH_3 and H_2O for a growth at 650°C is shown on the figure; a PH_3 concentration 2–3 times larger is used for growth at 700°C.

The process of obtaining low impurity levels by baking the growth solution is still a matter of some mystery. We note here some observations from our work. First, in order to routinely reduce the net impurity level, $N_D - N_A$, to the $(1–2) \times 10^{15}$ cm^{-3} level and to achieve electron mobilities in the 50,000–70,000 $cm^2/V \cdot s$ range at 77 K, growth at ~700°C is preceded by a bake of 50 h or more at about the same temperature and with ~0.7 ppm of added H_2O [11]. Second, we have achieved these results with indium from four sources [12]. However, each source was verified by mass spectrographic analysis to contain impurities at no higher than the 1 ppm level. Third, the purity of the graphite is important. A mass spectrographic analysis of graphite used in an apparatus that failed to produce high purity material showed 150 ppm of S, whereas that used to

* The work was sponsored by the Department of the Air force and the Department of the Navy.

0022-0248/81/0000–0000/$02.50

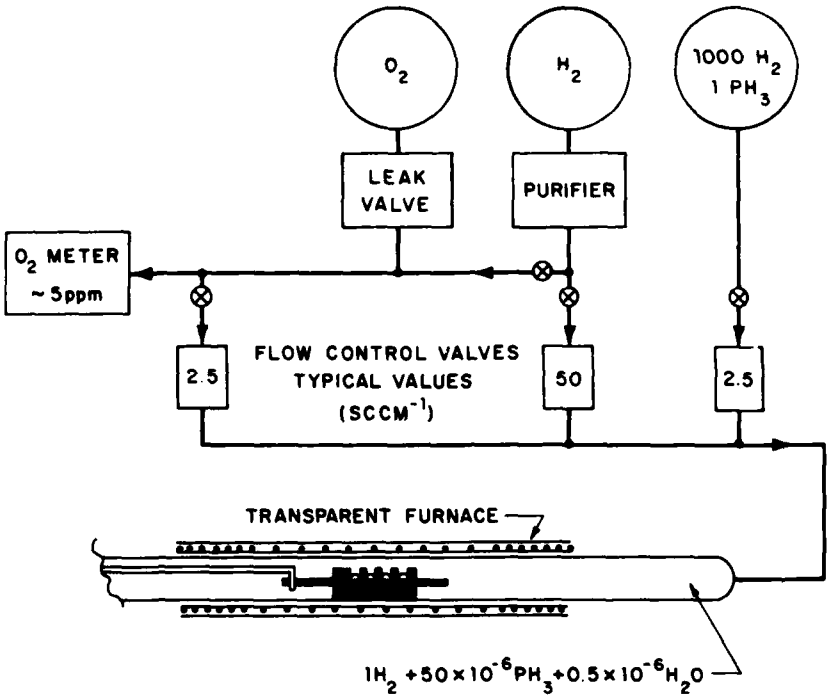

Fig. 1. LPE growth system schematic.

grow high purity material had about 1 ppm of S. We have used high purity graphite from two manufacturers [13] with comparable mass spectrograph and growth results.

The final point about the purity of LPE material is that the simple silicon contamination model apparently does not apply below the 1×10^{15} cm^{-3} level. In fig. 2 calculated silicon donor concentrations are shown as a function of H_2O pressure and temperature [11]. For our standard bake procedure, described above, the silicon concentration in the grown material should be about 1×10^{15} cm^{-3}, which is in good agreement with the measured values of $N_D - N_A$. However, the model also predicts that raising the H_2O pressure to 2×10^{-6} atm or decreasing the bake/growth temperature to 650°C should lower the silicon concentration to the 1×10^{14} cm^{-3} level. In fact, recent experiments have indicated that neither of these lowers $N_D - N_A$, and raising the H_2O pressure to 2×10^{-6} atm causes the mobility to decrease, indicating increased compensation. (It might be conjectured that reducing the bake/growth temperature from 700 to 650°C produces no change in $N_D - N_A$ because the reduced silicon concentration in the growth solution is offset by an increased silicon distribution coefficient. However, evidence that the distribution coefficient does not vary rapidly with temperature comes from the observation that for growths from unbaked solutions $N_D - N_A$, $\simeq 1 \times 10^{16}$ cm^{-3}, is independent of growth temperature in the 650–700°C range.)

A characteristic of high purity InP and InGaAsP grown by LPE is that it shows evidence of thermal activation of electrons from a deep level to the conduction band at temperatures above 250 K [14]; this is in addition to the usual thermal activation from shallow donors. Figs. 3 and 4 show the inverse Hall coefficient vs inverse temperature for InP and an InGaAsP alloy, respectively. The main figure shows the low-field Hall data which vary with temperature primarily because of electrons transferring to the conduction band from a shallow donor. The variation

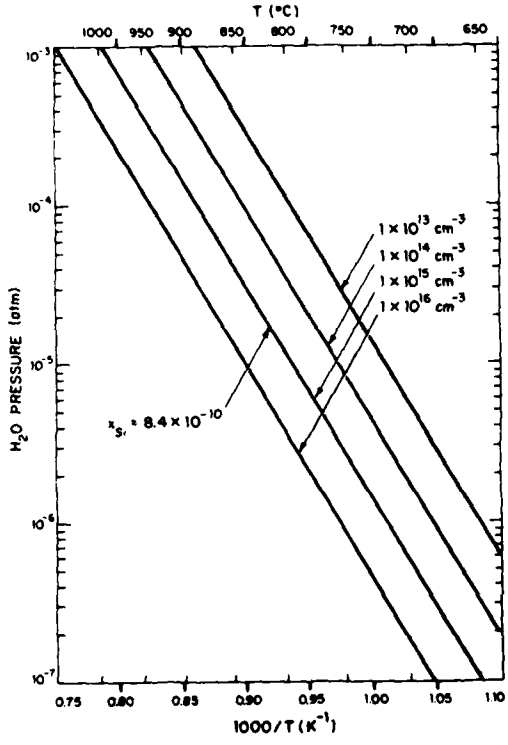

Fig. 2. Calculated lines of constant x_{Si} labeled by donor concentration in LPE InP for a Si distribution coefficient of 30.

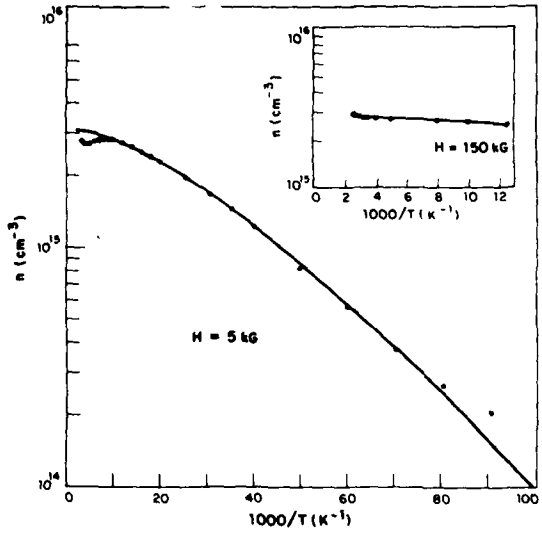

Fig. 3. Effective electron carrier concentration versus $1000/T$ for InP. Solid curve is calculated using $E_D = 3.7$ meV. Inset shows high-magnetic-field data; curve is calculated using deep-level concentration of 5×10^{15} cm^{-3} and energy of 0.29 eV.

of electron concentration at high temperatures is obscured by the changes in the Hall scattering factor as the scattering mechanism changes from primarily that of ionized impurity scattering to primarily that of polar-mode lattice scattering [15]. In this region it is necessary to measure the Hall coefficient in the high-field limit to determine the true dependence of electron concentration on temperature. Data taken at 150 kG, well within the high-field regime, are shown in the insets. The extra electron concentration at temperatures above 250 K, though small on the scale of the insets, has been observed for the many LPE-grown samples measured. In fig. 5 the high-temperature, high-magnetic field Hall data are plotted for an InP sample with a somewhat lower carrier concentration than that of fig. 3, and, consequently, the increased concentration due to the deep donors is more noticeable.

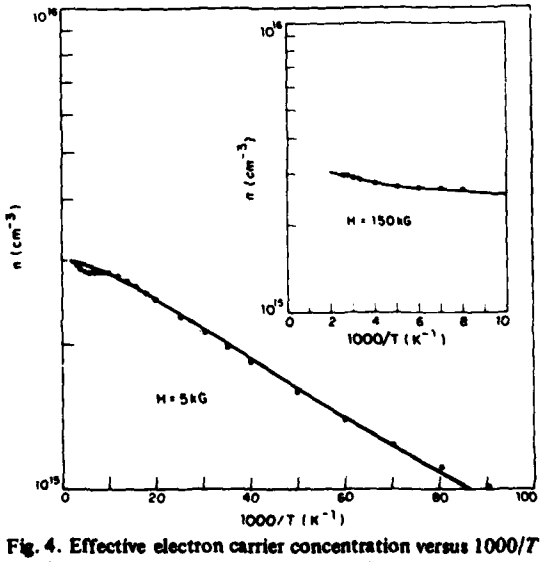

Fig. 4. Effective electron carrier concentration versus $1000/T$ for $In_{0.8}Ga_{0.2}As_{0.5}P_{0.5}$. Solid curve is calculated using $E_D = 0$. Inset shows high-magnetic-field data; curve is calculated using a deep-level concentration of 3×10^{14} cm^{-3} and energy of 0.12 eV.

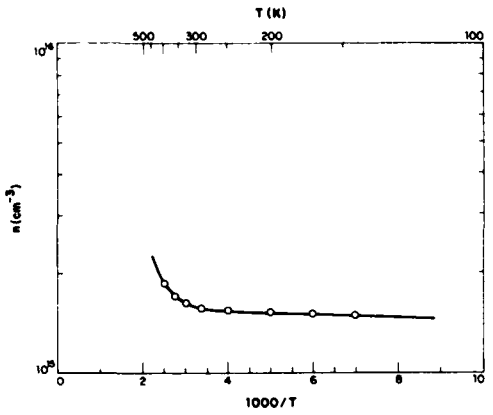

Fig. 5. Effective electron carrier concentration for another InP sample from measurements made at $H = 150$ kG. The solid curve is calculated with the same deep level parameters as in fig. 3 but a lower net carrier concentration.

Photoluminescence spectra of InP and the same InGaAsP alloy [16] are shown in figs. 6 and 7. Three peaks are observed; the highest energy peak is attributed to band-to-band transitions, and the lowest, together with a peak not shown at 0.35 eV, are probably due to transitions involving the 2^{2+} impurity level. The intermediate energy peak, in InP, was previously identified as being in most LPE samples and in the bottom portions of undoped, melt-grown crystals but absent in vapor-phase epitaxy [17]. The extra electron concentration above 250 K can be accounted for by taking the energy difference between the band-to-band and the intermediate peaks as the energy of the deep level. For InP this is 0.29 eV, and a concentration of 5×10^{15} cm^{-3} of this level is needed; for the InGaAsP alloy the energy is 0.12 eV, and a concentration of 3×10^{14} cm^{-3} is required. The reduced concentration of deep levels for the alloy in comparison to the InP is in qualitative agreement with the amplitudes of the respective photoluminescence peaks.

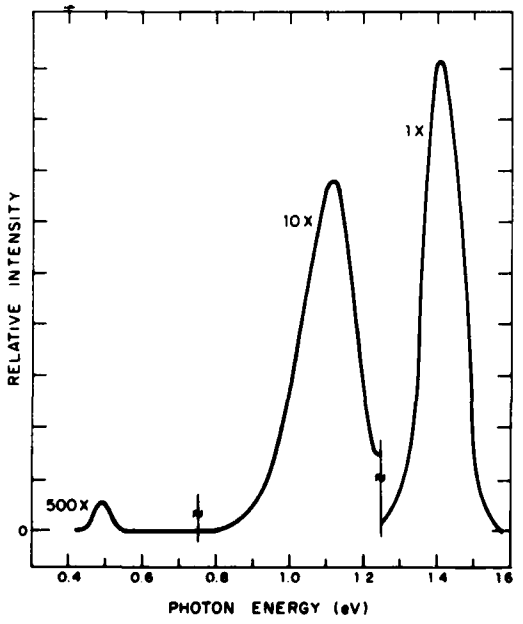

Fig. 6. Photoluminescence spectrum at $T \simeq 77$ K for undoped InP grown by LPE.

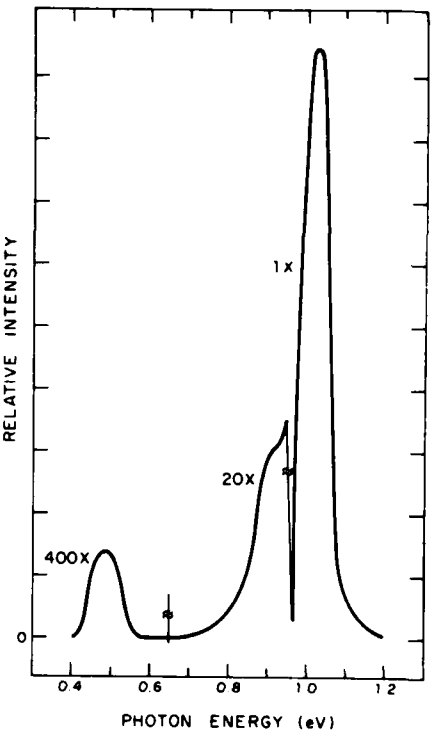

Fig. 7. Photoluminescence spectrum at $T \simeq 77$ K for undoped alloy of $In_{0.8}Ga_{0.2}As_{0.5}P_{0.5}$ grown by LPE.

The prominence of the intermediate peak for LPE material has led to speculation that it is associated with a phosphorus vacancy, in combination with

another impurity [17]. Yu recently has observed phonon structure on this line and fit it with a configuration coordinate model [18]. It is not yet clear whether or not his model is compatible with the ground state 0.2–0.3 eV below the conduction band that is needed to fit the electron concentration vs temperature data.

Two other observations were made relative to the deep levels discussed above. First, the extra electron concentration above 250 K was not detected for bulk InP of comparable purity grown by the liquid encapsulated Czochralski technique. Second, for LPE samples this concentration is not changed by the thermal annealing process reported by Eastman at this conference, although the concentration of shallow levels in InP is reduced by the annealing. Neither shallow nor deep level concentrations in InGaAsP samples are affected by the annealing process.

We have studied the effects of substrate orientation on surface morphology. Both InP and InGaAsP have been grown on substrates of (110) orientation. The InP grows well, probably with the best morphology of the three high symmetry directions, but the InGaAsP does not. The InGaAsP growth tends to form (111) facets, rather than to follow the (110) surface.

The second series of studies was motivated by Messham and Majerfeld's determination of the critical orientation for (100) and (111) surfaces [19]. According to Rode's theory [20], when there is terraced growth the tread of the terrace will be at the singular orientation, e.g. (100), and the riser will be at the critical orientation, which is at a small angular deviation from the singular orientation. In this situation the growth morphology will be greatly improved over that on nominally-oriented (100) sub-

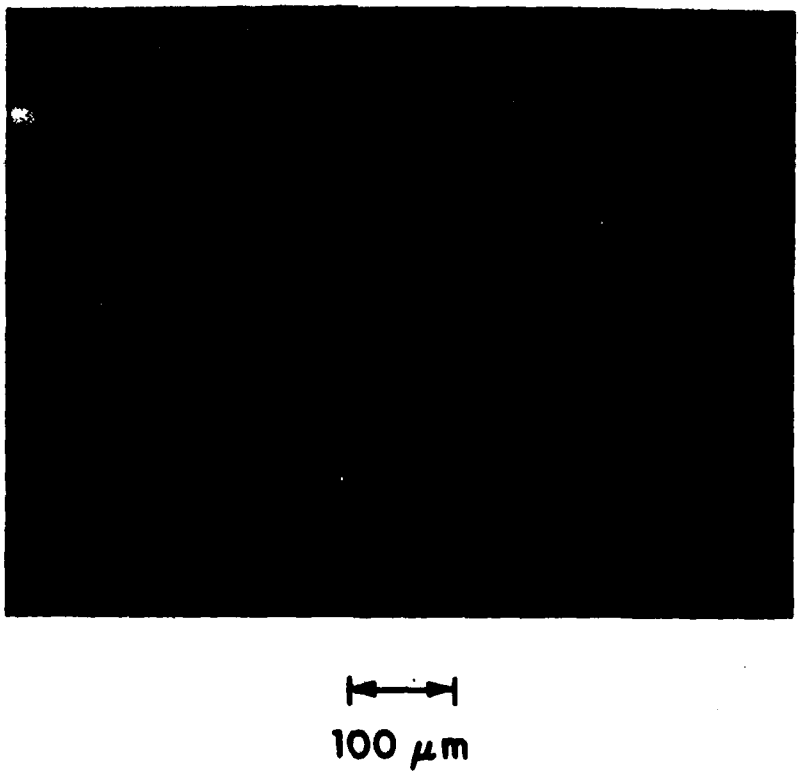

Fig. 8. Photomicrograph of InP LPE growth on a nominally oriented ( ) substrate.

strates by either orienting the substrate accurately to the singular direction or nominally orienting it to the critical orientation. We have prepared substrates oriented 2.6° off (100) toward a ⟨110⟩ direction, the critical orientation determined by Messham and Majerfeld, to test for improved morphology. Fig. 8 is a photomicrograph of a LPE layer of InP with morphology not untypical of that obtained for undoped or Sn-doped growth on a nominally oriented (100) substrate. From the picture it is unclear whether or not the structure on the surface is related to terracing. Apparently it is not, because we have found that there is little if any improvement when similar growths are made on critically oriented substrates. Also, growth on substrates closely oriented to the exact (100) (within 0.1°) is unchanged. Toyoda et al. [21] observed for LPE growth of GaAs that even small amounts of supercooling eliminate the terracing, and a similar effect may occur for InP.

An exception to this occurs for heavily Zn-doped InP growth. Fig. 9a shows growth of a layer with $N_A = 5 \times 10^{17}$ cm^{-3} in which terracing is quite evident. Fig. 9b shows growth of the same material on a substrate oriented 2.6° off (100) toward a ⟨110⟩ direction, and the change in morphology is quite striking. Apparently the critical orientation is at a slightly greater angle, and the terracing should be eliminated altogether for growth on that orientation. There are two notes of caution on the use of the critically oriented substrates. First, the background roughness in fig. 9b is due to the etchback under indium prior to growth. The indium etching does not work as well on the critically oriented substrates as on the nominally oriented (100) surfaces. However, with PH_3 in the atmosphere to prevent thermal etching, the indium etch before growth is unnecessary. Second, if the angle deviates too much from (100), nucleation problems occur (as seen by island growth). This has sometimes been observed at sample edges where rounding in substrate preparation or during the indium etching causes too large an angular deviation.

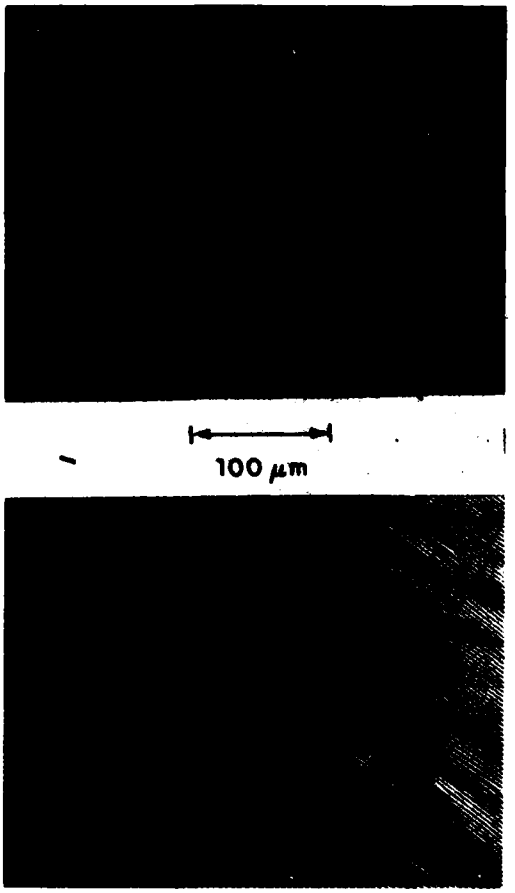

Fig. 9. (a) Photomicrograph of InP (Zn), $N_A = 5 \times 10^{17}$ cm^{-3}, grown by LPE on a nominally oriented (100) substrate. (b) Same as (a) except substrate is oriented 2.6° off (100) toward a ⟨110⟩ direction.

Acknowledgements

We wish to thank G.W. Iseler for providing the crystals for substrates. E.M. Swiggard of the Naval Research Laboratory has given us zone refined indium for impurity studies. J.G. Mavroides and D.F. Kolesar were collaborators in making the photoluminescence measurements. E.B. Owens carried out the mass spectrographic analyses of indium and graphite. W. DiNatale and J.M. Lawless have assisted in preparation of samples for transport measurements. Finally, we thank the staff of the Bitter National Magnet Laboratory for help with the high field measurements.

References

[1] J.J. Hsieh, J.A. Rossi and J.P. Donnelly, Appl. Phys. Letters 28 (1976) 709.

[2] C.E. Hurwitz and J.J. Hsieh, Appl. Phys. Letters 32 (1978) 487.

[3] V. Diadiuk, S.H. Groves and C.E. Hurwitz, Appl. Phys. Letters 37 (1980) 807.

[4] D.Z. Tsang, J.N. Walpole, S.H. Groves, J.J. Hsieh and J.P. Donnelly, Appl. Phys. Letters 38 (1981) 120.

[5] G.W. Turner, J.C.C. Fan and J.J. Hsieh, 14th IEEE Photovoltaic Specialists Conf., 1980.

[6] C.A. Armiento, S.H. Groves and C.E. Hurwitz, Appl. Phys. Letters 35 (1979) 333.

[7] K. Alavi, R.L. Aggarwal and S.H. Groves, Phys. Rev. B21 (1980) 1311.

[8] C.A. Burrus, A.G. Dentai and T.P. Lee, Electron. Letters 15 (1979) 656.

[9] Trans-Temp Co., Chelsea, MA, USA.

[10] A.R. Clawson, W.Y. Lum and G.E. McWilliams, J. Crystal Growth 46 (1979) 300.

[11] S.H. Groves and M.C. Plonko, in: Proc. 7th Intern. Symp. on GaAs and Related Compounds, St. Louis, 1978, Inst. Phys. Conf. Ser. 45 (Inst. Phys., London, 1979) p. 71.

[12] Cominco – zone refined by E.M. Swiggard of the Naval Research Laboratory, Indium Corporation of America, Johnson Matthey and MCP Electronics.

[13] POCO Graphite Inc. and Ultra Carbon Corp.

[14] Solid State Research Report, Lincoln Laboratory, MIT (1978: 4) p. 8, DDC AD-A068563/6.

[15] G.E. Stillman, C.M. Wolfe and J.O. Dimmock, J. Phys. Chem. Solids 31 (1970) 1199.

[16] Solid State Research Report, Lincoln Laboratory, MIT (1978: 4) p. 10, DDC AD-A068563/6.

[17] J.B. Mullin, A. Royle, B.W. Straughan, P.J. Tufton and E.W. Williams, J. Crystal Growth 31/14 (1972) 640.

[18] P.W. Yu, Solid State Commun. 34 (1980) 183.

[19] R. Messham and A. Majerfeld, Electronic Materials Conf., Boulder, CO, 1979.

[20] D.L. Rode, Phys. Status Solidi (a) 32 (1975) 425.

[21] N. Toyoda, M. Mihara and T. Hara, Japan. J. Appl. Phys. 18 (1979) 2207.

UNCLASSIFIED

SECURITY CLASSIFICATION OF THIS PAGE *(When Data Entered)*

REPORT DOCUMENTATION PAGE		READ INSTRUCTIONS BEFORE COMPLETING FORM
1. REPORT NUMBER ESD-TR-81-283	2. GOVT ACCESSION NO. AD-A112 878	3. RECIPIENT'S CATALOG NUMBER
4. TITLE *(and Subtitle)* Electrooptical Devices		5. TYPE OF REPORT & PERIOD COVERED Semiannual Technical Summary 1 October 1980 – 31 March 1981
		6. PERFORMING ORG. REPORT NUMBER
7. AUTHOR*(s)* Charles E. Hurwitz		8. CONTRACT OR GRANT NUMBER*(s)* F19628-80-C-0002
9. PERFORMING ORGANIZATION NAME AND ADDRESS Lincoln Laboratory, M.I.T. P.O. Box 73 Lexington, MA 02173		10. PROGRAM ELEMENT, PROJECT, TASK AREA & WORK UNIT NUMBERS Program Element Nos. 62702F and 61102F Project Nos. 2306 and 4600
11. CONTROLLING OFFICE NAME AND ADDRESS Rome Air Development Center Griffiss AFB, NY 13440		12. REPORT DATE 31 March 1981
		13. NUMBER OF PAGES 46
14. MONITORING AGENCY NAME & ADDRESS *(if different from Controlling Office)* Electronic Systems Division Hanscom AFB Bedford, MA 01731		15. SECURITY CLASS. *(of this report)* Unclassified
		15a. DECLASSIFICATION DOWNGRADING SCHEDULE

16. DISTRIBUTION STATEMENT *(of this Report)*

Approved for public release; distribution unlimited.

17. DISTRIBUTION STATEMENT *(of the abstract entered in Block 20, if different from Report)*

18. SUPPLEMENTARY NOTES

None

19. KEY WORDS *(Continue on reverse side if necessary and identify by block number)*

electrooptical devices	proton bombardment	ion implantation
avalanche photodiodes	double-heterostructure	GaInAsP/InP lasers

20. ABSTRACT *(Continue on reverse side if necessary and identify by block number)*

This report covers work carried out with the support of the Rome Air Development Center during the period 1 October 1980 through 31 March 1981.

The spectral dependence of the optical absorption introduced in InP and GaInAsP by proton bombardment has been measured as a function of dose. The induced absorption, which increases nearly linearly with dose, extends well beyond the band edge and decreases approximately exponentially with wavelength over a broad range. A short 420°C anneal reduces this bombardment-induced absorption by more than a factor of 10.

DD FORM 1 JAN 73 1473 EDITION OF 1 NOV 65 IS OBSOLETE

UNCLASSIFIED

SECURITY CLASSIFICATION OF THIS PAGE *(When Data Entered)*

20. ABSTRACT *(Continued)*

A study has been made of the etching technique used to delineate the active GaInAsP layer in GaInAsP/InP double-heterostructure lasers. It was found that careful control of etch solution compositions and etch time was necessary to obtain accurate measurement of active layer thickness.

A new method has been demonstrated for the prevention of thermal etching or decomposition of InP substrates prior to liquid-phase-epitaxial (LPE) growth. With this method the substrate is stored in the growth tube at room temperature during the pregrowth bake and then is transferred to the LPE slider shortly before growth. This method allows both high purity ($n \approx 1 \times 10^{15}$ cm^{-3}) and excellent surface morphology to be simultaneously and reproducibly obtained for both InP and GaInAsP LPE-grown layers.

High-quality n^+-InP layers over InGaAs have been grown from Sn solutions. The technique is generally applicable to the growth of an alloy of very low As content over one of high As content. The ability to grow these layers may facilitate the fabrication of improved InGaAs lasers and detectors operating at 1.55 μm.

attenuation is reduced by more than a factor of 10, to a level for the InP sample comparable to a bombardment of 0.033 D and for the GaInAsP sample comparable to a dose of approximately 0.05 D. This anneal corresponds to the heat treatment typically used for alloying ohmic contacts in our fabrication of proton-defined stripe-geometry lasers [5]. It is therefore significant that this heat treatment greatly reduces $\Delta\alpha$ in the

Semiconductors and Semimetals, vol. 3. New York: Academic, 1967, p. 153.
[10] M. Feng, T. H. Windhorn, M. M. Tashima, and G. E. Stillman, "Liquid-phase epitaxial growth of lattice-matched InGaAsP on (100)-InP for the 1.15–1.31-μm spectral region," *Appl. Phys. Lett.*, vol. 32, pp. 758–761, June 1978.
[11] R. H. Kingston, "Electroabsorption in GaInAsP," *Appl. Phys. Lett.*, vol. 34, pp. 744–746, June 1979.
[12] F. J. Leonberger, unpublished.